Records of Natural Products

www.acgpubs.org
ORIGINAL ARTICLE

Delving into the phytochemical constituents and biological activities of *Scorzonera coriacea* extracts: new perspectives from *in vitro* and *in silico* studies

Gunes Ak[1], Sakina Yagi[2], Mehmet Veysi Cetiz[3], Ramazan Tutus[4], Maria J. Rodrigues[5], Eliana Fernandes[5], Luisa Custodio[5], Evren Yildiztugay[6], Shaza H. Aly[7], Omayma A. Eldahshan[8,9], Abdel Nasser B. Singab[8,9] and Gokhan Zengin[1*]

[1]Department of Biology, Science Faculty, Selcuk University, Konya, Türkiye
[2]Department of Botany, Faculty of Science, University of Khartoum, Khartoum, Sudan
[3]Department of Medical Biochemistry, Faculty of Medicine, Harran University, Sanliurfa 63290, Türkiye
[4]Department of Molecular Biology and Genetics, Faculty of Engineering and Natural Sciences, Uşak University, 64200, Uşak, Türkiye
[5]Centre of Marine Sciences, Faculty of Sciences and Technology, University of Algarve, Campus of Gambelas, Faro, Portugal
[6]Department of Biotechnology, Science Faculty, Selcuk University, Konya, Türkiye
[7]Department of Pharmacognosy, Faculty of Pharmacy, Badr University in Cairo (BUC), Cairo, 11829, Egypt
[8]Pharmacognosy Department, Faculty of Pharmacy, Ain Shams University, Cairo, 11566, Egypt
[9]Center for Drug Discovery Research and Development, Ain Shams University, Cairo, Egypt

Abstract: The current study was designed to investigate the chemical composition, antioxidant, enzyme inhibitory, and cytotoxic activities of *Scorzonera coriacea* A.Duran & Aksoy. Both organs were rich in total phenolic content, with the highest content recorded from the 70% EtOH (48.41 mg GAE/g) and aqueous (47.11 mg GAE/g) extracts of the roots. All aerial parts extracts accumulated higher total flavonoid content than their respective roots extracts, with the highest amount found in their EtOH extract (36.44 mg RE/g). Chemical analysis revealed the presence of 86 compounds belonging to organic acids, phenolic acids, flavonoids, coumarins, anthocyanins, terpenes, saponins, and fatty acids and their derivatives, with the aerial parts accumulating the highest number. The roots displayed the strongest antiradical and ion-reducing capacities. EtOH extract of both organs recorded the highest acetylcholinesterase activity (2.77 and 3.02 mg GALAE/g; $p \geq 0.05$), while that of the root showed the best butyrylcholinesterase activity (3.49 mg GALAE/g) and that of the aerial parts the best tyrosinase inhibitory (59.07 mg KAE/g). EtOAc of the root exhibited the best cytotoxicity towards the HepG2 cell line (cell viability = 29.30%), but was also toxic towards HEK293 cells (cell viability = 11.72%). In silico screening supported these findings by identifying multiple strong ligand–protein interactions. Molecular dynamics simulations further confirmed the structural stability of selected complexes. In silico profiling docked 26 phytochemicals against 14 therapeutic targets, generating 364 complexes, of which 62% showed $\Delta G \leq -7.0$ kcal·mol^{-1}. Binding energies ranged from −1.4 to −10.7 kcal·mol^{-1}, with PD-1–Eriodictyol-7-O-neohesperidoside the best. For metabolic enzymes, Eriodictyol-7-O-neohesperidoside yielded the top α-amylase score and Diosmetin-7-O-glucoside the top α-glucosidase score, while several flavonoids bound AChE/BChE strongly; in contrast, tyrosinase displayed poor affinity overall. 100-ns MD simulations on five top complexes indicated stable behavior for C1 and C4, whereas C2/C3/C5 showed loosening interactions over time. These findings showed that *S. coriacea* could be a promising source of bioactive compounds with potential therapeutic applications.

Keywords: *Scorzonera coriacea*, molecular docking, molecular dynamics, antioxidant, enzyme inhibition, cytotoxicity

Cite this article as:
Ak et al. Delving into the phytochemical constituents and biological activities of *Scorzonera coriacea* extracts: new perspectives from *in vitro* and *in silico* studies. (2026). *Records of Natural Products*, 20(1):e25093633

Received: *10 September 2025*
Revised: *01 November 2025*
Accepted: *03 November 2025*
Published: *20 November 2025*

*Corresponding Author: Gokhan Zengin.
Email: gokhanzengin@selcuk.edu.tr

1 Introduction

The genus *Scorzonera* (Asteraceae family) comprises approximately 200 species, distributed in central and southern Europe, Asia, and northern Africa. *Scorzonera* species are caulescent perennial herbs that grow mainly in arid areas (Seyis et al., 2025). Many species are used as food and animal fodder, for rubber production, and in traditional medicine, such as for pulmonary and kidney conditions, wound healing, diabetes, and rheumatic pain (Şahin et al., 2023). A recent review reported that *Scorzonera* species are rich in diverse phytochemicals, including terpenes, steroids, quinic-acid derivatives, flavonoids, and phenylpropanoids. Pharmacologically, they possess anti-inflammatory, antinociceptive, wound-healing, anticancer, hepatoprotective, antimicrobial, antiulcerogenic, antidiarrheal, and antidiabetic activities, among others (Ak et al., 2020a; Dall'Acqua et al., 2020a, 2020b; Şahin et al., 2020b; Idoudi et al., 2023; Sarimahmut, 2023; Gong et al., 2024). Clinical applications indicated that some species are effective in treating herpes zoster and pregnancy resistance (Gong et al., 2024). Furthermore, various studies have documented the existence of biologically active compounds such as hyperoside, rutin, isoquercitrin, chlorogenic acid, luteolin, and cynarosidase in species belonging to the *Scorzonera* genus (Erez et al., 2022; Sarıaltın & Acıkara, 2022; Ajebli et al., 2025; Özcan Aykutlu et al., 2025). However, only about one-third of *Scorzonera* species have been examined for their chemistry and potential biological activity.

Türkiye is an important center of diversity for *Scorzonera* species. About 59 species are reported, of which 31 are endemic (Seyis et al., 2025). *S. coriacea*, an endemic species of Türkiye, is considered a distinct *Scorzonera* species without any close relatives. The species grows mainly in serpentine areas in the Konya district and Isparta province, Southern Anatolia, Türkiye. Morphologically, it has a thick, cylindrical rootstock, clearly clothed with the remains of old leaf bases; glabrous, hollow stems and distinct coriaceous, glabrous to sparsely tomentulose leaves; flowers are yellow and achenes are rigid and furrowed (Duran et al., 2011). A recent study revealed that the species is rich in flavonoids like hyperoside, isoquercitrin, rutin, and orientin, as well as caffeoylquinic acid derivatives, and it possesses significant antiradical activity (Sarıaltın & Acıkara, 2022). This study provides a comprehensive investigation of the chemical composition and the enzyme-inhibitory and cytotoxic activities of different extracts from the aerial parts and roots of *S. coriacea*. The antioxidant activity of extracts was highlighted by examining their capacity to scavenge free radicals, chelate and reduce metal ions, while their ability to inhibit enzymes was evaluated against enzymes implicated in diabetes, skin hyperpigmentation, and Alzheimer's disease. Their cytotoxicity was tested against the human embryonic kidney (HEK) 293, hepatocellular carcinoma (HepG2), and human neuroblastoma SHSY5Y cell lines. Despite encouraging pharmacological findings, the specific molecular interactions between the phytochemicals of *S. coriacea* and therapeutic targets remain to be elucidated. In the present study, molecular docking and molecular dynamics (MD) simulations were employed to evaluate the binding behavior of 26 major compounds against a set of standard enzymes involved in common metabolic and neurodegenerative diseases, as well as key oncogenic proteins such as AKT1, CDK2, CDK4, PD-1, TERT, and others, which are known to be overexpressed in HepG2 hepatocellular carcinoma cells. These in silico approaches are intended to clarify the potential multi-target inhibitory mechanisms of *S. coriacea* constituents and provide a molecular basis for their biological effects observed in earlier experimental assays.

2 Materials and Methods

2.1 Plant Collection

In 2023, a collection of plant samples was made in Konya (Derebucak, Camlık Location) at an altitude of 1560 meters in Türkiye. The botanical identification of the collected specimens was meticulously performed by Dr. Evren Yildiztugay. For documentation and future reference, a voucher sample was deposited in the herbarium of the Faculty of Science at Selcuk University (voucher number: EY3399). To preserve their phytochemical profile, the aerial parts of the plant were carefully separated post-harvest and air-dried in a shaded area at environmental temperature. Once dried, the material was finely powdered using a standardized grinding procedure. The powdered samples were subsequently stored in light-resistant containers under controlled environmental conditions to minimize degradation and maintain long-term stability.

2.2 Extraction Protocol

The extraction of bioactive components was performed using ethyl acetate, ethanol, ethanol/water (70%), and water. A standard 10-gram sample quantity was processed with 200 mL of each solvent. The protocol differed based on the solvent: organic extractions involved 24-hour maceration at room temperature, while the water-based method used a brief 15-minute hot water infusion. For post-processing, the aqueous extract was dehydrated by freeze-drying, and the organic solvents were evaporated under reduced pressure using rotary evaporation.

2.3 Assay for Total Phenolic and Flavonoid Content

The determination of total phenolic and flavonoid levels in the extracts was carried out based on previously established protocols (Zengin et al., 2016). All experimental details are given in the supplemental materials.

2.4 UHPLC–MS/MS Analysis of Polyphenolic Compounds

Phytochemical profiling followed a previously reported UHPLC–ESI–MS/MS method using high-performance liquid chromatographic (HPLC) analysis joined with an ESI-MS/MS spectrometer detector (El-Nashar et al., 2025). All chromatographic details are given in the supplemental materials.

http://doi.org/10.25135/rnp.2509.3633
Rec. Nat. Prod. 2026, 20(1):e25093633

2.5 Quantification of Selected Phenolic

The Thermo ORBITRAP Q-EXACTIVE mass spectrometer, which was equipped with a trifluoroacetic acid-treated C18 column (150 × 2.1 mm inner diameter, 3.5 µM particle size), was used to analyse the content of phenolic compounds in the tested extracts using LC–HRMS analysis (Han et al., 2018; Bursal et al., 2020; Kınoğlu et al., 2024; Özer et al., 2024; Karta et al., 2025). The LC-MS/MS parameters and validation data are given in the supplemental material.

2.6 Assays for *In vitro* Antioxidant Capacity

Antioxidant evaluations were conducted in accordance with established procedures, as delineated in a previous study (Grochowski et al., 2017). The radical scavenging capacities of the extracts were measured using a variety of assays, including FRAP, CUPRAC, DPPH, and ABTS. The results were expressed as milligrams of trolox equivalents (TE) per gram of dried extract. The total antioxidant potential was subsequently determined using the phosphomolybdenum (PBD) assay and reported in mmol TE/g. Furthermore, the metal chelation activity (MCA) was quantitatively assessed by measuring the milligrams of EDTA equivalents (EDTAE) per gram of extract. All experimental details are given in the supplemental materials.

2.7 Inhibitory Effects Against Some Key Enzymes

Enzyme inhibitory assays were conducted against acetylcholinesterase (AChE), butyrylcholinesterase (BChE), tyrosinase, amylase, and glucosidase using the tested extracts, according to validated protocols reported in the literature (Grochowski et al., 2017). The inhibitory activities toward AChE and BChE were subsequently quantified in milligrams of galanthamine equivalents (GALAE) per gram of dry extract. The inhibitory potential of amylase and glucosidase was expressed in acarbose equivalents (ACAE), while tyrosinase inhibition was assessed in terms of kojic acid equivalents (KAE) per gram of dry extract. All experimental details are given in the supplemental materials.

2.8 Cell Culture and Cell Viability Assessment

Human hepatocarcinoma (HepG2), human neuroblastoma (SH-SY5Y), and human embryonic kidney (HEK 293) cells were maintained as previously detailed (Rodrigues et al., 2016). The cells were seeded into 96-well plates at densities of 5,000 cells per well. After an overnight incubation, the cells were exposed to extracts at 100 µg/ml for 72 hours. Cells treated with 0.5% DMSO served as the control group. Cell viability was measured using the MTT assay (3-(4,5-dimethylthiazol-2-yl)-2,5-diphenyltetrazolium bromide), as previously described by Rodrigues et al. (2016). Viability percentages were calculated in comparison to the DMSO control (0.5%).

2.9 Computational Study

2.9.1 Molecular Docking

Comprehensive molecular docking analyses were conducted to evaluate the binding affinities of major phytochemicals derived from *S. coriacea* against a wide range of biologically significant targets. These included key metabolic enzymes, such as α-glucosidase (7KBJ), tyrosinase (6QXD), butyrylcholinesterase (6EQP), and acetylcholinesterase (7E3H), as well as regulatory and signaling proteins that exhibited high levels of expression in hepatic cell lines (Chiavaroli et al., 2023; Llorent-Martínez et al., 2025; Yagi et al., 2025). The following genes have been identified: AKT (4GV1), BRPF1 (5MWZ), CDK2 (6GUE), CDK4 (2W96), Cyclin D1 (2W99), MYC (1NKP), PPARγ (1I7I), PD-1 (5N2F), and (TERT) (5CQG) (Rosenberry et al., 2017). Docking simulations were performed using AutoDock Vina v1.1.2 with an exhaustiveness level of 32 (Dileep et al., 2022). POCASA v1.1 was used to predict binding sites and define grid boxes. The coordinates and dimensions of each grid box used in the docking simulations are provided in Table S1 (Zengin et al., 2025). To ensure the accuracy of the docking outcomes, we conducted re-docking of native ligands and RMSD evaluations (Baloglu et al., 2025; Yildirim et al., 2025). We characterized the resulting protein–ligand interactions using the Protein–Ligand Interaction Profiler (PLIP), which identified hydrogen bonds, hydrophobic contacts, and π-interactions (Angeles Flores et al., 2024; Cetiz et al., 2024). The final binding poses and interaction networks were visualized using PyMOL v3.0.

2.9.2 Molecular Dynamics Simulations

To explore the conformational flexibility and thermodynamic stability of the protein–ligand complexes, molecular dynamics (MD) simulations were performed using GROMACS 2023.3 (Cetiz et al., 2025). Each simulation featured one of the top-docked phytochemicals from *S. coriacea* bound to proteins. The simulation systems were constructed using the CHARMM-GUI web server (Jo et al., 2008; Korpayev et al., 2025) employing the CHARMM36m force field for proteins and the CHARMM General Force Field (CGenFF) for ligands (Maier et al., 2015). The complexes were solvated in a cubic TIP3P water box with a minimum 10 Å margin from any solute atom and neutralized with Na^+ and Cl^- ions at a physiological concentration of 0.15 M. Energy minimization was carried out using the steepest descent algorithm until the maximum force on the system was reduced below 1000 kJ mol^{-1} nM^{-1}. After minimization, two equilibration steps were executed. Equilibration comprised 500 ps under NVT, followed by 1 ns under NPT at 310 K. It was observed that all bond lengths were constrained using the LINCS algorithm. The long-range electrostatics were calculated using the Particle Mesh Ewald (PME) method with a real-space cutoff of 12 Å. In contrast, the Verlet cutoff scheme was applied for short-range nonbonded interactions. To facilitate a comprehensive evaluation of structural dynamics and binding stability, production MD trajectories were executed for 100 ns per complex.

2.10 Statistical Analysis

The experiments were conducted three times, and the variations among the extracts were assessed through One-way ANOVA utilizing Tukey's test, with the analysis conducted

using GraphPad Prism (version 9.2). A p-value of under 0.05 was considered statistically significant.

3 Results and Discussion

3.1 Total Phenolics (TPC) and Flavonoids (TFC) Contents

The TPC and TFC of different extracts from the aerial parts and roots of *S. coriacea* were determined, and the results are presented in Table 1. The TPC extracts from the aerial parts ranged between 22.14 and 42.57 mg GAE/g, and in those from the roots, between 22.76 and 48.41 mg GAE/g. The highest content was recorded from the 70% EtOH and aqueous extracts from the roots ($p \geq 0.05$), followed by the 70% EtOH of the aerial parts, while the EtOAc extract of both organs recovered the least content. The TFC in aerial parts extracts ranged from 5.34 to 36.44 mg RE/g, while those from the roots ranged from 0.91 to 5.58 mg RE/g. The highest TFC was recorded respectively from EtOH, 70% EtOH, and aqueous extracts from the aerial parts. All aerial parts extracts accumulated higher TFC than their respective root extracts. The highest content in the roots, which was comparable to that in the EtOAc extract of the aerial parts, was obtained from the EtOH and aqueous extracts ($p \geq 0.05$). It was noted that polar solvents with hydroxyl groups, such as water and ethanol, are more effective in recovering solid mass from vegetal matrices. Furthermore, the combination of solvents with different polarities could increase the bioactive compound extraction efficiency. Certainly, other factors, including the chemical nature of the phytochemicals, the particle size of the sample, and the existence of interfering compounds, can significantly influence the recovery of metabolites (El Kamari et al., 2024). These results supported a previous study indicating that both organs were rich in TPC and TFC (Sarıaltın & Acıkara, 2022). The authors indicated that the methanol/water extract of *S. coriacea* contains total phenolic contents of 53.32 mg GAE/g in its aerial parts and 52.24 mg GAE/g in its roots.

The total phenolic and flavonoid contents in various *Scorzonera* species have been documented by numerous researchers. Notably, Idoudi et al. (2023) analyzed *S. undata* extracts using ultrasound-assisted and maceration methods, finding their total phenolic content to range from 0.66 to 26.97 mg GAE/g, which are lower values compared to those in this study. Şahin et al. (2020b) reported total phenolic levels between 26.8 and 124.3 mg GAE/g in ethyl acetate, chloroform, and n-butanol fractions derived from the ethanolic extract of *S. pygmaea* aerial parts. Ayromlou et al. (2020) found that the methanol extract of *S. calyculata* had a total phenolic content of 4.69 mg GAE/g. Our findings for total phenolic content align with literature values for other *Scorzonera* species, such as *S. hieracifolia* (aerial parts: 19.40–40.88 mg GAE/g; roots: 17.50–26.11 mg GAE/g) (Dall'Acqua et al., 2020a) and *S. hispanica* (aerial parts: 13.02–37.68 mg GAE/g; roots: 9.65–25.31 mg GAE/g) (Ak et al., 2020b). Differences in phenolic content among *Scorzonera* species may be due to geographic and climatic influences, as well as the extraction methods or solvents employed.

Table 1. Total phenolic (TPC) and flavonoid (TFC) contents in extracts from aerial parts and roots of *Scorzonera coriacea*

Parts	Extracts	TPC (mg GAE/g)	TFC (mg RE/g)
Aerial parts	EtOAc	22.14±0.29^{d}	5.34±0.40^{d}
	EtOH	39.86±0.22^{c}	36.44±0.35^{a}
	70% EtOH	42.57±0.31^{b}	18.53±0.16^{b}
	Water	39.02±0.23^{c}	13.67±0.25^{c}
Roots	EtOAc	22.76±0.81^{d}	0.91±0.03^{f}
	EtOH	39.17±0.63^{c}	5.58±0.07^{d}
	70% EtOH	48.41±1.50^{a}	4.22±0.08^{e}
	Water	47.11±0.26^{a}	5.19±0.02^{d}

Note: Values are reported as mean±SD of three parallel measurements. GAE: Gallic acid equivalent; RE: Rutin equivalent. Different letters indicate significant differences between the tested extracts ($p < 0.05$).

3.2 UPLC/MS Analysis of Different Extracts of S. coriacea Aerial Parts and Roots

Ultra-performance liquid chromatography coupled with tandem mass spectrometry (UPLC/MS) was used to tentatively describe the phytoconstituents of the different extracts (Ethyl acetate, ethanol, ethanol/water, and water) from *S. coriaceum* aerial parts (SCA) and roots (SCR) in both the negative and positive ion modes (Figures supplementary material).

The results revealed a diverse array of phytochemicals, highlighting the plant's rich chemical composition and potential pharmacological significance. The study identified 85 compounds across various classes, including phenolic acids, flavonoids, fatty acids, coumarins, triterpenoids, and others, with distinct distribution patterns between the aerial parts and roots, as well as among different extraction solvents (Ethyl acetate, ethanol, ethanol/water, and water). Table 2 presents the characterized compounds, including their molecular ions, fragment ions, and corresponding chemical classes. The metabolites were identified by comparing retention times, mass spectral data, and fragmentation patterns with previously reported information (Aly et al., 2024a; Cusumano et al., 2024). The findings indicated that the characterized metabolites encompass many phytochemical groups, including phenolic acids and their derivatives, flavonoids, fatty acids and amides, along with triterpenoids, coumarins, and anthocyanins. The flavonoids and fatty acid amides were the most prominent classes of detected compounds in both SCA and SCR. This comparative phytochemical characterization represents the first study on *S. coriacea* conducted by UPLC/MS analysis.

3.2.1 Flavonoids

A wide range of flavonoids, including flavanols (e.g., myricetin, taxifolin), flavone glycosides (e.g., apigenin and luteolin derivatives), and flavonol glycosides (e.g., quercetin and kaempferol derivatives), were identified. Notably, quercetin and kaempferol (Peaks 58 and 30, respectively) were detected in multiple extracts, underscoring their significance as major bioactive constituents. Twenty-three chromatographic peaks were identified as flavonoid

http://doi.org/10.25135/rnp.2509.3633
Rec. Nat. Prod. 2026, 20(1):e25093633

Table 2. The UPLC-ESI/MS-MS based characterization of phytoconstituents of the different extracts of *S. coriacea* aerial parts and roots in negative and positive ionization modes (–: absent)

Peak no.	t_R	$[M-H]^-$	$[M+H]^+$	MS^2	Tentatively identified compounds	Phytochemical class	Aerial parts				Roots				Ref.
							EtOAc	EtOH	EtOH/Aq.	Aq.	EtOAc	Ethanol	EtOH/Aq.	Aq.	
							Presence								
1	0.63	341.14	–	179	Sucrose	Sugar	–	–	–	–	–	+	+	+	Dall'Acqua et al. (2020a)
2	0.65	317.16	–	133, 191, 213, 272	Myricetin	Flavanol	–	–	–	+	–	–	+	–	Abdl Aziz et al. (2024)
3	0.69	191.15	–	173, 153, 130	Quinic acid	Organic acid	+	–	+	+	–	–	+	–	Goher et al. (2024)
4	0.72	377.09	381.00	353, 191, 179, 161, 119, 341	Quinic acid derivative	Phenolic acid	–	+	–	+	–	+	+	–	Cusumano et al. (2024)
5	0.77	439.07	–	179	Caffeic acid derivative	Phenolic acid	–	–	–	–	–	–	–	+	Dall'Acqua et al. (2020a)
6	1.14	191.08	–	111, 129, 173	Citric acid	Organic acid	–	–	–	–	–	–	–	+	Magdy et al. (2024)
7	1.45	353.03	–	191	3-O-Caffeoylquinic acid	Phenolic acid	–	–	–	–	–	+	+	–	Dall'Acqua et al. (2020a)
8	2.37	707.47	–	353, 191	3-O-Caffeoylquinic acid dimer	Phenolic acid	–	+	+	+	–	–	–	+	Dall'Acqua et al. (2020a)
9	2.50	–	163.07	145, 135, 117	Umbelliferone	Coumarin	–	+	+	+	–	–	+	+	Khattab et al. (2023)
10	2.51	353.32	–	191	5-O-Caffeoylquinic acid	Phenolic acid	–	+	+	+	–	–	–	+	Dall'Acqua et al. (2020a)
11	5.07	465.36	–	259, 107, 285, 179, 151	Taxifolin-3-O-hexoside	Flavanol glycoside	–	+	–	–	+	–	+	+	Goufo et al. (2020)
12	5.11	–	305.06	287, 259, 231, 153, 149, 123, 153	Taxifolin (Dihydroquercitin)	Flavanol	–	–	–	–	–	+	+	–	Khattab et al. (2023)
13	5.54	563.06	–	396, 443, 353, 269	Apigenin 6-C-hexoside-8-C-pentoside	Flavone glycoside	–	+	–	–	–	–	–	–	Cusumano et al. (2024)
14	5.59	447.07	–	239, 327, 284	Luteolin-C-hexoside (Isoorientin)	Flavone glycoside	–	+	–	–	–	–	–	–	Granica et al. (2015)
15	5.73	461.11	–	313, 299, 284, 256, 227, 188	Disometin-O-hexoside	Flavone glycoside	–	+	–	–	–	–	–	–	Dall'Acqua et al. (2020a)
16	5.98	609.00	–	300, 271, 463, 151	Quercetin deoxyhexoside-O-hexoside (Quercetin-3-O-rutinoside)	Flavonol glycoside	–	+	–	+	–	–	–	–	Granica et al. (2015)
17	6.02	431.15	433.13	355, 311, 431, 271, 169, 125	Kaempferol 3-deoxyhexoside (Afzelin)	Flavonol glycoside	–	+	+	–	–	–	–	–	Atasagun et al. (2025)
18	6.21	463.06	–	301, 417, 277,327, 271, 225, 169	Quercetin-O-hexoside	Flavonol glycoside	–	–	–	–	–	+	+	–	Dall'Acqua et al. (2020a)
19	6.27	–	163.03	154, 145, 132, 134, 119, 107	Hydroxycoumarin	Coumarin	–	–	–	–	–	–	+	–	Khattab et al. (2023)
20	6.3	447.14	–	411, 357, 327, 297, 284, 278	Orientin (Luteolin-C-hexoside)	Flavone glycoside	–	+	–	–	–	–	–	–	Dall'Acqua et al. (2020a)
21	6.34	–	305.56	249, 251, 228, 173	Dihydroquercitin	Flavanol	–	–	–	–	–	–	–	+	Khattab et al. (2023)

Table 2. (Continued)

Peak no.	t_R	$[M-H]^-$	$[M+H]^+$	MS^2	Tentatively identified compounds	Phytochemical class	Aerial parts				Roots				Ref.
							EtOAc	EtOH	EtOH/Aq.	Aq.	EtOAc	Ethanol	EtOH/Aq.	Aq.	
							Presence								
22	6.77	447.23	–	285, 257, 217, 151	Kaempferol-O-hexoside	Flavonol glycoside	–	+	–	–	–	–	–	–	Dall'Acqua et al. (2020a)
23	6.82	515.21	–	353, 191, 179	3,5-O-Dicaffeoylquinic acid	Phenolic acid	–	+	–	+	–	+	+	+	Granica et al. (2015)
24	6.84	–	493.20	331	Malvidin-3-hexoside	Anthocyanin	–	+	–	–	–	–	–	–	Magdy et al. (2024)
25	6.89	343.20	–	267, 203, 177, 135	Eupatorin	Flavone	–	+	–	–	–	–	–	–	Zengin et al. (2022)
26	6.91	–	163.07	135, 117	Hydroxycoumarin	Coumarin	–	–	–	–	–	+	–	–	Khattab et al. (2023)
27	6.93	515.35	–	353, 179, 85	1,3 O-Dicaffeoylquinic acid	Phenolic acid	–	–	+	–	–	–	–	–	Dall'Acqua et al. (2020a)
28	7.17	343.20	–	315, 299, 285, 253, 225	Dihydroxytrimethoxyflavone	Flavone	–	+	–	–	–	–	–	–	Zengin et al. (2022)
29	7.34	–	153.09	153, 110, 60	Vanillin	Phenolic aldehyde	–	–	–	+	–	–	–	–	Atasagun et al. (2025)
30	7.90	285.00	–	257, 217, 199, 151	Kaempferol	Flavonol	+	+	+	+	–	–	–	–	Dall'Acqua et al. (2020a)
31	8.78	327.31	–	229, 206, 155, 291, 211, 183, 171, 99	Trihydroxy octadecadienoic acid	Fatty acid	+	–	+	+	–	–	–	–	Farag et al. (2016b)
32	8.94	–	301.20	286, 287, 259, 229, 169	3,5,7-Trihydroxy-4′-methoxyflavone (Diosmetin)	O-Methylated flavone	–	–	–	+	–	–	–	–	Magdy et al. (2024)
33	9.36	329.22	353.17 $[M+Na]^+$	229, 211, 171, 183, 99, 245, 157	Trihydroxy- octadecenoic acid	Fatty acid	+	+	+	+	+	+	+	+	AbouZeid et al. (2022)
34	9.65	–	181.18	163, 135	Caffeic acid	Phenolic acid	–	+	–	–	–	–	–	–	Granica et al. (2015)
35	10.01	793.47	–	631, 485	Dihydroxy-23-oxo-12-oleanen-28-oic acid-O-deoxyhexosyl-hexoside	Triterpenoid Saponin	–	–	–	–	–	+	+	–	Zengin et al. (2024)
36	10.13	309.17	–	291, 253, 191	Eicosaenoic acid	Fatty acid	+	+	+	–	–	–	–	–	Zengin et al. (2024)
37	10.41	327.32	–	113, 215, 257, 269, 301, 318	Trihydroxy-octadecadienoic acid	Fatty acid	–	–	–	–	+	–	–	+	Farag et al. (2016b)
38	10.65	307.14	–	217, 185, 99	Eicosadienoic acid	Fatty acid	+	–	–	–	–	–	–	–	Zengin et al. (2022)
39	10.69	–	291.48	273, 245, 151, 139	Catechin	Flavanol	+	–	–	–	–	–	–	–	Khattab et al. (2023)
40	10.94	647.34	–	485	Dihydroxy-23-oxo-12-oleanen-28- oic acid-O-hexoside	Triterpenoid Saponin	–	–	–	–	–	+	+	–	Zengin et al. (2024)
41	11.57	–	274.55	106, 256, 274	Hexadecasphinganine	Sphingolipid	–	–	+	–	–	–	–	–	Cusumano et al. (2024)
42	11.59	293.29	–	275, 249, 195, 113. 97	9-Oxo-(10*E*, 12*Z*)-octadecadienoic acid	Fatty acid	–	–	+	–	–	–	–	–	Granica et al. (2015)
43	11.78	327.10	–	301, 233, 284, 174, 128	Dihydroxy-oxo-12-octadecenoic acid	Fatty acid	–	–	–	–	–	–	–	+	Farag et al. (2013)
44	11.98	311.44	–	293, 267, 171, 153	Dihydroxy-linoleic acid	Fatty acid	+	–	–	+	–	–	–	–	Farag et al. (2016b)

http://doi.org/10.25135/rnp.2509.3633
Rec. Nat. Prod. 2026, 20(1):e25093633

Table 2. (Continued)

Peak no.	t_R	$[M-H]^-$	$[M+H]^+$	MS^2	Tentatively identified compounds	Phytochemical class	Aerial parts				Roots				Ref.
							EtOAc	EtOH	EtOH/Aq.	Aq.	EtOAc	Ethanol	EtOH/Aq.	Aq.	
							Presence								
45	12.93	–	295.95	169, 155, 141, 121, 107, 81	13-Hydroxy-octadecatrienoic acid	Fatty acid	–	+	–	–	–	–	–	–	Granica et al. (2015)
46	13.13	311.43	–	293, 153	Dihydroxy-linoleic acid	Fatty acid	+	–	–	–	–	–	–	–	Zengin et al. (2024)
47	14.17	–	280.28	263, 165, 119, 107/194, 199	Octadecadienoic acid amide	Fatty acid amide	–	+	–	–	–	+	+	–	Farag et al. (2016b)
48	14.23	293.24	–	249, 211, 183, 171, 121, 109	13-Oxo-(9*Z*, 11*E*)-octadecadienoic acid	Fatty acid	+	–	+	–	–	–	–	–	Granica et al. (2015)
49	14.43	293.28	–	275, 249, 197, 185, 125	13-Oxo-(9*E*, 11*E*)-octadecadienoic acid	Fatty acid	+	–	+	–	–	–	–	–	Granica et al. (2015)
50	14.72	–	280.31	263, 165, 119, 107, 109	Octadecadienoic acid	Fatty acid	+	+	+	+	+	+	+	–	AbouZeid et al. (2022)
51	14.98	595.2	–	289, 593, 594, 561, 268	Eriodictyol-7-O-neohesperidoside	Flavanone glycoside	–	–	–	–	–	–	+	–	Magdy et al. (2024)
52	15.11	475.49	–	209, 167, 123	Vanillin deoxyhexose-O-hexoside	Aldehyde glycoside	–	–	–	–	+	–	–	–	Khattab et al. (2023)
53	15.14	311.11	–	293, 235, 119, 108, 149, 102	Octadecenedioic acid	Fatty acid	–	–	–	–	+	–	+	–	Farag et al. (2016a)
54	15.16	–	280.28	105, 109, 133	Octadecadienoic acid	Fatty acid	+	–	–	–	–	–	–	–	AbouZeid et al. (2022)
55	15.39	–	297.30	295, 277, 179, 171, 141	Hydroxy octadecadienoic acid (Hydroxy-linoleic acid)	Fatty acid	–	+	+	–	–	+	+	–	Zengin et al. (2024)
56	15.42	295.26	297.30	277, 183	Hydroxy octadecadienoic acid (Hydroxy-linoleic acid)	Fatty acid	+	–	+	–	+	+	–	–	Granica et al. (2015)
57	15.53	311.19	–	295, 261, 217, 128	Octadecenedioic acid	Fatty acid	–	–	–	–	+	–	+	–	(Farag et al., 2016a)
58	15.66	–	303.29	303, 285, 257, 165, 153, 137	Quercetin	Flavonol	+	–	–	–	–	–	–	–	Dall'Acqua et al. (2020a)
59	15.9	293.17	–	275, 249, 197, 185, 125	13-Oxo-(9E,11E)-octadecadienoic acid	Fatty acid	+	–	–	–	+	–	–	–	Granica et al. (2015)
60	16.55	–	561.45	339, 309, 293, 435, 418/543, 307, 245, 175	Linoleic acid dimer	Fatty acid	–	+	–	–	–	–	–	–	Khattab et al. (2023)
61	16.61	297.13	299.5	279, 274, 253, 171	Hydroxy octadecenoic acid (Hydroxy-oleic acid)	Fatty acid	+	–	–	–	+	–	–	–	Ayoub et al. (2021)
62	17.01	313.34	–	255, 225	Dihydroxydimethoxyflavone	Flavone	+	–	–	–	–		–	–	Zengin et al. (2022)
63	17.19	–	228.31	43, 57, 74, 88, 102, 144, 187	Myristamide	Fatty acid amide	+	+	+	–	+	+	+	–	Zengin et al. (2024)
64	17.28	295.33	–	277, 183	Hydroxy octadecadienoic acid isomer	Fatty acid	+	–	–	–	–	–	–	–	Granica et al. (2015)
65	18.56	311	–	293, 291, 201	Octadecenedioic acid isomer	Fatty acid	–	–	+	–	–	–	–	+	Farag et al. (2016a)

Table 2. (Continued)

Peak no.	t_R	$[M-H]^-$	$[M+H]^+$	MS^2	Tentatively identified compounds	Phytochemical class	Aerial parts				Roots				Ref.
							EtOAc	EtOH	EtOH/Aq.	Aq.	EtOAc	Ethanol	EtOH/Aq.	Aq.	
							Presence								
66	18.64	–	280.35	109, 133	Octadecadienoic acid isomer	Fatty acid	+	+	+	+	+	+	+	+	Cusumano et al. (2024)
67	19.61	271.35	–	180	Hydroxypalmitic acid	Fatty acid	–	–	+	–	–	–	–	–	Farag et al. (2016a)
68	19.69	517.33	–	485, 385, 205, 198, 167	Sinapic acid-O-hexosidepentoside	Phenolic acid	–	–	–	–	+	–	–	–	Farag et al. (2022)
69	20.16	–	256.29	163, 102, 144, 130	Palmitamide	Fatty acid amide	+	+	+	+	+	+	+	+	Zengin et al. (2024)
70	20.30	339.27	–	299, 251, 179	Caffeoyl hexoside	Phenolic acid	–	–	+	–	–	–	–	–	Dall'Acqua et al. (2020a)
71	20.65	–	282.33	241, 121, 109, 111	Oleamide	Fatty acid amide	+	+	+	+	–	+	+	+	Zengin et al. (2024)
72	20.78	473. 47	–	451, 380, 246	Dimethoxy hydrocinnamic acid	Phenolic acid	–	–	–	–	+	–	–	–	Khattab et al. (2023)
73	20.92	313.27	–	183	Dihydroxy-octadecenoic acid	Fatty acid	+	–	–	–	–	–	–	–	Farag et al. (2014)
74	21.11	–	282.33	107, 111, 149, 163	Oleamide	Fatty acid amide	+	–	+	+	–	–	–	–	Zengin et al. (2024)
75	21.38	–	609.49	591, 577, 549, 532, 491, 485, 459, 253/325	Disometin-O-deoxyhexosied, O-hexoside (Diosmin)	Flavone	+	+	–	–	–	–	–	–	Magdy et al. (2024)
76	21.59	–	282.12	107, 111, 149, 163	Oleamide	Fatty acid amide	+	–	–	–	+	–	–	–	Zengin et al. (2024)
77	21.98	–	593.29	533, 329, 359, 431, 449, 463, 561	Luteolin-C-hexoside-O-dideoxy hexoside-methyl ether	Flavone	+	+	+	–	–	–	–	–	Farag et al. (2016b)
78	22.52	–	593.25	533, 459, 374, 346, 406, 447, 478	Isovitexin-4′-O-deoxyhexoside-7-methyl ether	Flavone	–	+	–	–	–	–	–	–	Farag et al. (2016a)
79	22.53	327.24	–	–	Hydroxyoctadecenedioic acid	Fatty acid	+	–	–	–	–	–	–	–	Farag et al. (2016a)
80	23.19	–	284.35	107, 109, 102, 158, 116	Stearamide	Fatty acid amide	+	+	+	+	–	+	+	+	Zengin et al. (2024)
81	23.34	325.15	–	193, 161, 149, 134	Fertaric acid	Phenolic acid	–	–	–	–	+	–	–	–	Zengin et al. (2022)
82	23.64	–	284.31	102, 111, 135, 144	Stearamide	Fatty acid amide	+	–	+	–	–	+	–	–	Zengin et al. (2024)
83	24.08	499.33	–	539, 464, 256, 169, 377, 273, 163, 119	Caffeoyl-coumaroyl-quinic acid	Phenolic acid	–	–	–	–	+	–	–	–	Benayad et al. (2014)
84	24.45	471.34	–	410, 409, 451, 443, 427, 409	Hydroxylated triterpenoid acid	Triterpenoid	–	–	–	–	+	–	–	–	Dall'Acqua et al. (2020a)
85	25.18	471.16	–	409, 430, 427, 409	Hydroxy-betulinic acid	Triterpenoid	–	–	–	–	+	–	–	–	Dall'Acqua et al. (2020a)

glycosides. Quercetin, luteolin, and kaempferol exhibited the predominant aglycone moieties in their glycosides. The identification of these glycosides was based on the elimination of sugar moieties, and an additional characteristic fragmentation pattern of aglycone via Retro-Diels–Alder (RDA). Additionally, free aglycones were identified in peaks 2 (*m/z* 317), 25 (*m/z* 343), and 39 (*m/z* 291) corresponding to myricetin, eupatorin, and catechin, respectively. Peak 30 (*m/z* 285) and peak 58 (*m/z* 301), corresponding to kaempferol and quercetin, respectively, are found in the aerial parts only. Flavanol at peaks 12, 21 (*m/z* 305) corresponding to dihydroquercitin in the roots only. Moreover, a dihydroxydimethoxyflavone and a dihydroxytrimethoxyflavone were identified at *m/z* $[M-H]^-$ 313 and $[M-H]^-$ 343.20, respectively. The ion mass peaks at *m/z* $[M+H]^+$ 291.48, $[M-H]^-$ 285.00, and $[M+H]^+$ 303.29 correspond to the aglycones catechin, kaempferol, and quercetin in the aerial parts only in the ethyl acetate fraction, and *m/z* $[M+H]^+$ 305.06 corresponds to dihydroquercetin in the roots only. Commonly, flavonoid glycosides are tentatively described through the removal of hexose moiety (162 amu) and deoxyhexose (146 amu) or pentoside moiety (132 amu) in their fragmentation spectra (Aly et al., 2024b; Zengin et al., 2024). They are predominantly present in the aerial parts rather than the roots, especially the ethyl acetate and ethanol fractions as taxifolin, kaempferol, diosmetin, malvidin, and luteolin hexoside and deoxyhexose glycosides. The flavonoid glycosides characterised in the roots are quercetin-O-hexoside and eriodictyol-7-O-neohesperidoside (Table 2). Consistent with our findings, quercetin, luteolin, and kaempferol glycosides were previously extracted from other *Scorzonera* species, including *S. hispanica* and *S. hieraciifolia* (Granica et al., 2015; Dall'Acqua et al., 2020a).

3.2.2 Phenolic Acids and Derivatives

Various phenolic compounds were prominently detected, with compounds such as quinic acid, caffeoylquinic acids, and their derivatives (e.g., 3-O-Caffeoylquinic acid, 5-O-Caffeoylquinic acid) being abundant in both aerial and root extracts. These compounds are known for their antioxidant and anti-inflammatory properties (Aly et al., 2023; Abdelazim et al., 2024), suggesting potential health benefits of *S. coriacea* extracts. They are characterized based on the loss of a water molecule and the carboxylate part (18 and 44 amu) in their fragmentation pattern. Peaks 3 are assigned as quinic acid $[M-H]^-$ at *m/z* 191 due to the presence of the dehydrated peak at *m/z* 173. Also, peak 4 at *m/z* 377 is characterized as a quinic acid derivative with the fragment of quinic acid loss at *m/z* 191. Different peaks identified 3-O-caffeoylquinic acid, 5-O-caffeoylquinic acid (peaks 7 and 10), and its dimer at (peak 8) were identified at *m/z* 353.03, 353.32, 707.47, respectively, which were previously identified in the methanolic extracts of *S. hieraciifolia* aerial parts and root extracts (Dall'Acqua et al., 2020a). All of these peaks were accompanied by distinct fragments at *m/z* 191, confirming loss of caffeic moiety. Two peaks (23 and 27) were characterized as 3,5- and 1,3-O-dicaffeoylquinic acid at *m/z* 515.21. Both peaks exhibited ion fragment peaks at 353 and 179, corresponding to mono caffeoylquinic acid and the loss of the quinic acid moiety, respectively (Zhang et al., 2018). Moreover, caffeic acid derivative (peak 34) was identified at *m/z* 181.18, accompanied by distinct fragments at *m/z* 135, confirming a CO_2 neutral loss (Zhang et al., 2018). Moreover, peaks 70 and 81 were identified as fertaric acid and caffeoyl hexoside at *m/z* 325.15 and 339.27, respectively. Interestingly, caffeic acid and 3,5-O-dicaffeoylquinic acid were previously reported in the subaerial parts of *S. hispanica* (Granica et al., 2015).

3.2.3 Fatty Acids and Amides

The chromatogram of SCA and SCR ethyl acetate fraction mostly revealed the presence of fatty acids, where 27 peaks were identified as fatty acids, such as trihydroxy-9,14-octadecadienoic acid, eicosaenoic acid, eicosadienoic acid, dihydroxy-linoleic acid, 13-oxo-(9*E*,11*E*)-octadecadienoic acid, and octadecadienoic acid. The long-chain fatty acids (saturated, mono-, and polyunsaturated) are eluted last in the chromatogram due to their lipophilic nature. Moreover, 8 peaks were identified as fatty acid amides, and they represent the major compounds identified in SCA and SCR, especially in the ethanol and ethyl acetate fractions. They were characterized as octadecadienoic acid amide, myristamide, palmitamide, oleamide, and stearamide at positive ion mode with molecular ion peaks at *m/z* 280.28, 228.31, 256.29, 282.33, and 284.35, respectively. The previous report revealed the presence of various fatty acids in the ethyl acetate extract of *S. hispanica* (Granica et al., 2015) and agrees with our results. In Turkish flora, myristamide, palmitamide, oleamide, and stearamide are among the predominant fatty acid amides (Nilofar et al., 2024; Zengin et al., 2024).

3.2.4 Miscellaneous

The hydroxycoumarin was annotated in the SCR alcoholic extracts represented as *m/z* $[M+H]^+$ 163.03, also umbelliferone was identified in both SCA and SCR alcoholic extracts as *m/z* $[M+H]^+$ 163.07, and agrees with previous reports for coumarins in *S. cretica* (Paraschos et al., 2001), *S. aucheriana* (Erik et al., 2021).

Few triterpenoids were identified in SCR ethyl acetate or ethanol extracts, including *m/z* 793.47, 647.34, 471.34, and 471.16 for dihydroxy-23-oxo-12-oleanen-28-oic acid-O-deoxyhexosyl-hexoside, dihydroxy-23-oxo-12-oleanen-28-oic acid-O-hexoside, hydroxylated triterpenoid acid, and hydroxy-betulinic acid, and in agreement with previous reports for triterpenoids in *S. hieraciifolia* (Dall'Acqua et al., 2020a).

The extraction efficiency exhibited considerable variation depending on the solvent applied. For example, EtOH and EtOH/Aq. Extracts exhibited a higher concentration of flavonoids and phenolic acids, while aqueous extracts were enriched with polar compounds such as sucrose and organic acids. The EtOAc extracts exhibited a higher concentration of fatty acids and flavonoids, including quercetin

and kaempferol. The roots demonstrated an elevated content of certain compounds, including sucrose and triterpenoid saponins, whereas the aerial parts were more abundant in flavonoids such as luteolin derivatives. This varied distribution may indicate the plant's tolerance to environmental stressors and could inform targeted extraction approaches for specific bioactive compounds.

The UPLC-ESI-MS/MS profiling of *S. coriacea* extracts underscores its potential as a source of bioactive compounds with diverse therapeutic applications. The solvent-dependent variation in compound distribution highlights the importance of optimizing extraction protocols for specific phytochemical classes. Future studies should focus on isolating and characterizing the major compounds to validate their biological activities through *in vitro* and *in vivo* assays. Additionally, comparative metabolomic studies with other *Scorzonera* species could further elucidate the chemotaxonomic and pharmacological uniqueness of *S. coriacea*.

The Venn diagram analysis showcases both the unique and shared chemical profiles derived from various solvent extractions of the plant's aerial and root sections. In the aerial part extracts (Figure 1), those obtained with ethanol (AP-EtOH) stood out by producing the highest number of unique compounds (n = 14), showcasing their superior dissolving capability for a broad array of phytochemicals. Notably, five compounds were consistently present across all AP extracts, implying the existence of fundamental metabolites, regardless of the solvent's polarity. A comparable pattern was seen in the root extracts (Figure B), where the ethyl acetate extract (R-EA) featured the most unique constituents (n = 9), highlighting its preference for semi-polar to non-polar compounds. The comparative two-way Venn diagrams between the aerial and root sections for each solvent (Figures C–F) indicated that, although some metabolites were common, each tissue displayed a unique phytochemical profile. For instance, AP-EtOH had 22 unique compounds compared to seven in R-EtOH, and AP-EA and R-EA shared only seven compounds but had 16 and 11 unique metabolites, respectively. Overall, these results suggest that the polarity of solvents and the type of plant tissue significantly affect both the extraction effectiveness and variety of secondary metabolites, emphasizing the critical role of careful solvent selection in phytochemical research.

3.3 Quantification of Selected Phenolic Compounds

We quantified selected phenolic compounds (apigenin-7-glucoside, apigenin, caffeic acid, luteolin-7-rutinoside, luteolin, orientin and quercetin) in the tested extracts. The results are shown in Table 3. In the extracts from the aerial parts of the plant, orientin was the main compound (150.0–2664.4 µg/g of extract), with the highest level found in the ethanol extract. Regarding the root extracts, the most abundant compound in the ethanol/water and water extracts was caffeic acid (13.3 and 13.2 µg/g, respectively), while the main component in the ethanol and ethyl acetate extracts was luteolin (19.80 and 2.6 µg/g, respectively). The levels of apigenin in the root extracts were below the limit of quantification (LOQ). Our findings are consistent with previous studies. For example, Ercan et al. (2024) reported significant levels of orientin in extracts from various *Scorzonera* species. Additionally, Sarıaltın and Acıkara (2022) detected orientin in the aerial parts of *S. sandrasica, S. coriacea* and S. *ahmet-duranii* extracts, but not in the root extracts. Similar fact was also reported by Xie et al. (2016) for *S. austriaca* and Ak et al. (2020a) for *S. hispaniaca*.

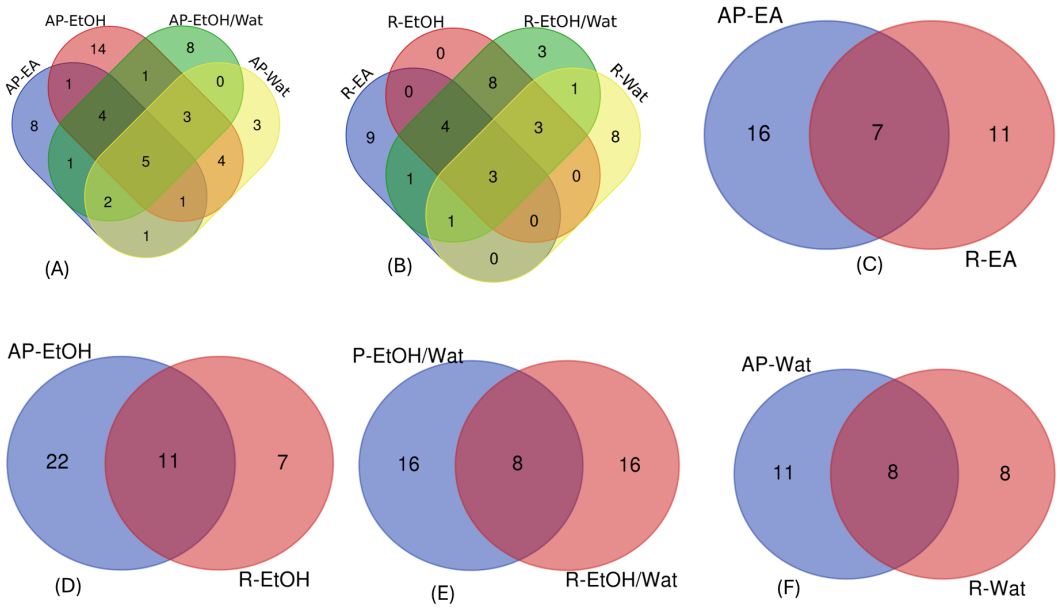

Figure 1. Venn diagrams based on the numbers of the identified compounds in the extracts. (A) Aerial parts extracts; (B) Root extracts; (C) Ethyl acetate extracts; (D) Ethanol extracts; (E) Ethanol/Water extracts; (F) Water extracts

http://doi.org/10.25135/rnp.2509.3633
Rec. Nat. Prod. 2026, 20(1):e25093633

Table 3. The quantification of some phenolic compounds in the tested extracts (μg/g)

Compound Name	Aerial parts				Roots				Relative uncertainty (Ux, %)
	EtOAc	EtOH	EtOH/Aq.	Aq.	EtOAc	EtOH	EtOH/Aq.	Aq.	
Apigenin-7-glucoside	72.6	593.9	269.0	16.7	1.3	3.1	3.9	<LOD	4.5
Apigenin	<LOQ	0.5	0.6	0.6	<LOQ	<LOQ	<LOQ	<LOQ	4.8
Caffeic acid	1.6	15.6	12.5	45.1	1.2	9.3	13.3	13.2	6.3
Luteolin 7-rutinoside	0.5	9.1	10.9	1.6	10.1	<LOD	1.0	0.6	3.7
Luteolin	42.3	133.8	113.8	62.3	2.6	19.8	2.3	<LOQ	5.7
Orientin	150.0	2664.4	1192.7	405.9	0.2	4.9	7.6	4.3	6.0
Quercetin	<LOQ	3.8	12.2	18.6	<LOQ	1.1	1.4	2.4	4.4

Note: LOQ: Limit of quantification; LOD: Limit of detection.

3.4 Antioxidant Activity

The antioxidant activity of different extracts from the aerial parts and roots of *S. coriacea* was determined using various assays. DPPH and ATBS assays (Mallikarjunaswamy et al., 2024) measure the ability of the extract to scavenge free radicals and FRAP and CUPRAC assays indicate the reducing capacity of the extract. In contrast, the phosphomolybdenum assay evaluates its effectiveness in reducing the Mo (VI) to (MoV). The metal chelating ability of the extract is determined by measuring its iron chelating ability. Results are presented in Table 4. The anti-DPPH activity ranged between 23.96 and 292.63 mg TE/g, with the highest activity recorded respectively from the 70% EtOH of the roots and aerial parts. Also, the EtOH and aqueous extracts from the roots showed strong DPPH radical-scavenging activity (269.89 and 272.27 mg TE/g, $p \geq 0.05$). ABTS radical-scavenging activity ranged between 35.38 and 379.90 mg TE/g, with both aqueous and 70% extracts of the roots revealing the highest activity ($p \geq 0.05$), followed by 70% EtOH extract (340.83 mg TE/g) of the aerial parts and EtOH extract (318.45 mg TE/g) from the roots. The ions' reducing activity was in the range of 76.06–393.82 mg TE/g in the CUPRAC assay and 34.02–224.57 mg TE/g in the FRAP assay. The three polar extracts displayed potent ion-reducing capacity, with the 70% EtOH extract of the roots exerting the highest effect, followed by its aqueous extract, and the 70% EtOH extract from aerial parts in the CUPRAC assay. EtOAc extract of both organs had the lowest values. The metal chelating activity ranged between 11.81 and 18.73 mg EDTAE/g, with the highest effect recorded from the 70% EtOH activity of aerial parts, followed by its aqueous extract. In comparison, the best activity from the root extracts was obtained from the aqueous and 70% EtOH extracts, which were comparable to the EtOH (16.36 mg EDTAE/g) and EtOAc extracts from the aerial parts. The total antioxidant activity of extracts ranged between 1.38–2.71 mmol TE/g, with the EtOAc and 70% EtOH extracts from the aerial parts recorded the highest effect ($p \geq 0.05$), followed by their EtOH extract and all root extracts, except their EtOH extract (2.14–2.33 mmol TE/g, $p \geq 0.05$). Overall, extracts from both organs displayed significant antioxidant activity in all assays, and the highest values for their antiradical and ion-reducing capacity were obtained from the roots. In contrast, those for their chelating and total antioxidant activity were obtained from the aerial parts. Many of the identified compounds in the present study, such as kaempferol (Deng et al., 2019), quercetin (Lesjak et al., 2018), orientin (Praveena et al., 2014), and their derivatives, caffeic and quinic acid and their derivatives (Tajner-Czopek et al., 2020; Islam et al., 2024), and umbelliferone (Lin et al., 2023), were known for their significant antioxidant activity. Variation in the antioxidant property of different extracts could be attributed to the amount of the antioxidant compounds as well as the presence of synergistic or antagonistic interactions of several compounds [68–70]. A previous study indicated that the aerial parts exerted higher anti-DPPH and anti-ABTS activities than the roots, contrary to the present findings (Sarıaltın & Acıkara, 2022). This variation could be associated with many factors, including factors associated with the plant itself (as genetic effects and age), environmental conditions (as climate and soil type) as well as extraction conditions. Also, stage of vegetation and flowering has an impact on the accumulation of metabolites in different organs of plants (Chakraborty et al., 2022). It is worth noting that the current study highlighting for the first time the antioxidant properties of *S. coriacea* using different assays and results indicated that the plant could be a promising source of antioxidant compounds.

The literature indicates that various *Scorzonera* species possess antioxidant properties. For instance, Idoudi et al. (2023) observed that ethanol extracts from different parts of *S. undulata* demonstrated greater activity than water extracts, aligning with our findings. Similarly, research by Dall'Acqua et al. (2020a) on *S. hieracifolia* revealed that both the aerial parts and roots exhibited higher antioxidant activities with methanol and water extracts compared to ethyl acetate extracts. These results were also found for *S. tomentosa* (Dall'Acqua et al., 2020b) and *S. hispanica* (Ak et al., 2020b). Conversely, Temiz (2021) noted that a 75% ethanolic extract of *S. cinerea* showed lower DPPH (0.46 mmol TE/g) and ABTS (0.07 mg TE/g) radical scavenging capabilities than those reported for ethanol/water extracts in this study. Additionally, Şahin et al. (2020a) discovered that the ethyl acetate fraction from the ethanol extract of *S. pygmaea* was more active in DPPH, ABTS, and FRAP assays compared to butanol and chloroform fractions. Furthermore, Harkati et al. (2010) reported that the methanol extract of *S. undulata*

Table 4. Antioxidant properties of extracts from aerial parts and roots of *Scorzonera coriacea*

Parts	Extracts	DPPH (mg TE/g)	ABTS (mg TE/g)	CUPRAC (mg TE/g)	FRAP (mg TE/g)	MCA (mg EDTAE/g)	PBD (mmol TE/g)
Aerial parts	EtOAc	23.96±0.43^{e}	38.71±0.70^{e}	76.06±3.95^{f}	34.02±1.03^{h}	14.86±0.07^{d}	2.71±0.07^{a}
	EtOH	50.59±0.09^{d}	83.66±0.22^{d}	213.70±3.63^{d}	114.80±1.08^{e}	16.36±0.20^{c}	2.14±0.20^{cd}
	70% EtOH	278.77±2.09^{b}	340.83±1.46^{b}	328.59±6.07^{b}	177.72±1.31^{c}	18.73±0.37^{a}	2.50±0.13^{ab}
	Water	52.08±0.07^{d}	92.13±0.24^{d}	168.22±1.29^{e}	106.83±1.29^{f}	17.59±0.20^{b}	1.38±0.02^{e}
Roots	EtOAc	27.14±1.33^{e}	35.38±0.28^{e}	84.40±4.29^{f}	43.85±0.99^{g}	12.58±0.51^{e}	2.24±0.04^{bc}
	EtOH	269.89±1.14^{c}	318.45±2.18^{c}	304.22±8.41^{c}	170.55±0.83^{d}	11.81±0.22^{f}	1.87±0.13^{d}
	70% EtOH	292.63±1.66^{a}	361.64±3.42^{a}	393.82±3.01^{a}	224.57±4.46^{a}	14.43±0.10^{d}	2.26±0.05^{bc}
	Water	272.27±2.71^{c}	379.90±18.44^{a}	331.46±3.38^{b}	195.44±0.59^{b}	15.85±0.06^{c}	2.33±0.02^{bc}

Note: Values are reported as mean±SD of three parallel measurements. TE: Trolox equivalent; EDTAE: EDTA equivalent; MCA: Metal chelating activity; PBD: Phosphomolybdenum. Different letters indicate significant differences between the tested extracts ($p < 0.05$).

ssp. *deliciosa* exhibited stronger DPPH radical scavenging activity than trolox, a standard compound. Most previous studies on the antioxidant capabilities of *Scorzonera* species found a direct correlation between total phenolic/flavonoid content and the antioxidant activities of the extracts tested. This suggests that phenolic compounds in the *Scorzonera* genus mainly contribute to their antioxidant properties.

3.5 Enzyme Inhibitory Activity

The enzyme inhibitory activity of different extracts from the aerial parts and roots of *S. coriacea* was determined against acetylcholinesterase (AChE), butyrylcholinesterase (BChE), tyrosinase (Tyr), α-amylase, and α-glucosidase enzymes, and the results are presented in Table 5. The anti-AChE activity ranged between not active and 3.02 mg GALAE/g with the highest effect exerted by the EtOH extract of both organs ($p \geq 0.05$), followed by the 70% EtOH extract from the root, while the EtOAc and 70% EtOH extracts from the aerial parts possessed comparable effect (2.19 and 2.22 mg GALAE/g; $p \geq 0.05$). The anti-BChE activity ranged between not active and 3.49 mg GALAE/g, with the EtOH extract from the roots showing the highest effect, followed by its 70% EtOH extract and the EtOAc extract from the aerial parts. Other extracts were either inactive or displayed a weak effect. All extracts could inhibit the Tyr (22.92–59.07 mg KAE/g), with the highest inhibitory effect displayed by the EtOH extract of the aerial parts, followed by the EtOH extract from the roots and the 70% EtOH extract of the two organs, which exerted comparable activity. The aqueous extract exerted the least tyrosinase inhibition activity. Extracts demonstrated superior effect on the α–glucosidase compared to the α-amylase, with the 70% EtOH extract from the roots and aerial parts exhibited respectively the highest effect (1.43 and 1.38 mmol ACAE/g; $p < 0.05$), followed respectively by the EtOH extract of the latter and that of the former (1.29 and 1.23 mmol ACAE/g; $p < 0.05$). The best inhibitory effect towards the α–amylase was exerted by the EtOAc extract of both organs (0.64 and 0.61 mmol ACAE/g; $p \geq 0.05$) while other extracts displayed weak inhibitory activity. Amylase and glucosidase inhibition is considered as one of the most effective strategy in the treatment of diabetes (Mahdi et al., 2024; Gladis et al., 2025).

To the best of our knowledge, this is the first report of the enzyme inhibitory properties of *S. scorpioides*. Additionally, little information is available regarding the enzyme-inhibitory properties of other *Scorzonera* species. For example, Ak et al. (2020a) reported on the inhibitory properties of various *S. hispanica* extracts, finding that water extracts were the most active against AChE (aerial parts: 2.35 mg GALAE; roots: 2.64 mg GALAE/g), while the same extracts exhibited the least activity against tyrosinase (aerial parts: 8.00 mg KAE/g; roots: inactive). In their study, n-hexane, ethyl acetate, and dichloromethane extracts displayed greater activity against amylase and glucosidase than methanol and infusion extracts. However, Dall'Acqua et al. (2020b) found that dichloromethane extracts of *S. tomentosa* (aerial parts: 2.57 mg GALAE/g; roots: 2.41 mg GALAE/g) displayed higher AChE inhibition than methanol and water extracts. Leaf extracts from *S. papposa, S. mollis*, and *S. semicana* were found to effectively suppress α-glucosidase [37]. Additionally, an in vivo study on *S. cinerea* revealed that the leaves exhibited a notable hypoglycaemic effect (Temiz, 2021). Therefore, the results of the present study suggest that, in addition to its antidiabetic effect, the *Scorzonera* species could play a significant role in the treatment of skin hyperpigmentation and Alzheimer's disease. However, some of the compounds identified in the current study were shown to have potential for inhibiting enzymes. For instance, kaempferol and quercetin exhibit anti-AChE (Liao et al., 2022; Shi et al., 2023), anti-Tyr (Shang Jin et al., 2011; Fan et al., 2017), and α-glucosidase inhibitory (Peng et al., 2016; Günal-Köroğlu et al., 2025) properties. Quinic acid was found to effectively inhibit the α-glucosidase enzyme (Han et al., 2024). An *in vivo* experiment found that taxifolin-3-O-hexoside lowered blood glucose levels, and an in silico study confirmed its potent antidiabetic potential (Gurumayum et al., 2023).

3.6 Multivariate Analysis

Recently, there has been a growing interest in multivariate statistical analysis for assessing complex datasets. This

http://doi.org/10.25135/rnp.2509.3633
Rec. Nat. Prod. 2026, 20(1):e25093633

Table 5. Enzyme inhibitory effects of extracts from aerial parts and roots of *Scorzonera coriacea*

Parts	Extracts	AChE (mg GALAE/g)	BChE (mg GALAE/g)	Tyrosinase (mg KAE/g)	Amylase (mmol ACAE/g)	Glucosidase (mmol ACAE/g)
Aerial parts	EtOAc	2.19±0.09^{c}	2.70±0.61^{b}	52.12±0.70^{c}	0.61±0.03^{a}	na
	EtOH	2.77±0.06^{ab}	0.37±0.07^{cd}	59.07±0.59^{a}	0.37±0.02^{b}	1.29±0.01^{c}
	70% EtOH	2.22±0.05^{c}	na	55.96±0.36^{b}	0.35±0.01^{b}	1.38±0.03^{b}
	Water	0.04±0.01^{e}	na	22.92±0.43^{d}	0.08±0.02^{d}	na
Roots	EtOAc	1.80±0.29^{d}	0.17±0.02^{d}	49.98±2.40^{c}	0.64±0.01^{a}	na
	EtOH	3.02±0.02^{a}	3.49±0.17^{a}	55.36±0.71^{b}	0.33±0.01^{bc}	1.23±0.01^{d}
	70% EtOH	2.67±0.04^{b}	2.26±0.23^{b}	55.60±0.58^{b}	0.30±0.01^{c}	1.43±0.01^{a}
	Water	na	0.93±0.14^{c}	23.42±0.25^{d}	0.09±0.02^{d}	0.96±0.03^{e}

Note: Values are reported as mean±SD of three parallel measurements. GALAE: Galantamine equivalent; KAE: Kojic acid equivalent; ACAE: Acarbose equivalent. na: not active. Different letters indicate significant differences between the tested extracts ($p < 0.05$).

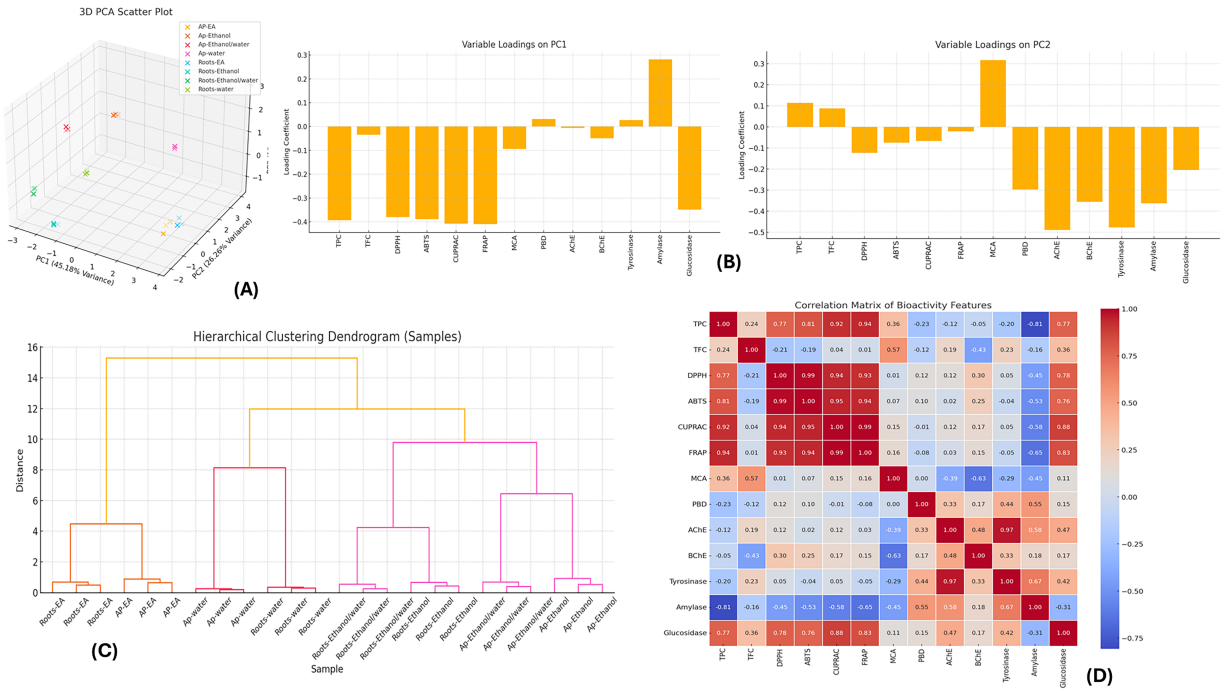

Figure 2. Multivariate analysis based on biological activity results. (A) 3D PCA scatter plot: (B) Variables in PC1 and PC2; (C) Hierarchical cluster analysis; (D) Pearson correlation analysis

analytical method has also been utilized to gain insights into various parameters within phytochemical studies. In this context, we conducted a multivariate analysis based on biological activity results. Initially, we carried out Pearson correlation analysis between the total bioactive components and biological activities, with findings presented in Figure 2. Notably, radical scavenging and reducing power abilities exhibited strong correlations with total phenolic content. Similarly, numerous studies have shown a linear relationship between total phenolic content and antioxidant properties. Conversely, PBD and MCA did not correlate with total phenolic content, which can be attributed to the presence of non-phenolic chelators such as peptides and polysaccharides.

Furthermore, no correlation was observed between total phenolic content and enzyme inhibitory effects. This suggests that the results may be influenced by the complex nature of phytochemicals or their interactions. To ascertain the distribution within the tested samples, a principal component analysis was performed, and the findings are summarized in Figure 2. The PCA explained 71.44% of the total variance (PC1: 45.18% and PC2: 26.26%). Ethanol and ethanol/water extracts were distinctly separated from ethyl acetate and water extracts, primarily due to the higher antioxidant potential of the ethanol/water extract. Significantly, PC1 was predominantly influenced by total phenolic content and antioxidant properties, whereas PC2 showed a strong correlation with enzyme inhibition (AChE, BChE, α-glucosidase, and tyrosinase). In conclusion, we suggest that hydroethanolic extraction may be advantageous for developing functional applications using *S. coriacea*.

Table 6. Cytotoxicity of extracts (at 100 µg/ml) from aerial parts and roots of *Scorzonera coriacea* on HEK 293, HepG2 and SHSY5Ycell lines

Parts	Extracts	HEK 293	HepG2	SHSY5Y
Aerial parts	EtOAc	10.73±2.44	36.28±1.87	89.15±5.65
	EtOH	30.63±6.12	62.67±3.03	101.48±6.81
	70% EtOH	42.18±6.86	67.63±4.86	106.44±3.47
	Water	99.35±4.3	77.61±4.61	114.19±2.41
Roots	EtOAc	11.72±1.44	29.3±1.21	86.1±4.97
	EtOH	75.48±1.34	64.83±3.15	103.69±2.93
	70% EtOH	120.67±3.62	88.02±3.52	110.22±4.27
	Water	116.7±5.85	94.58±3.91	110.64±3.62

Note: At least three experiments were performed in triplicate; n = 9.

3.7 Cytotoxicity

The cytotoxic effect of different extracts from the aerial parts and roots of *S. coriacea* against the Human embryonic kidney (HEK) 293, hepatocellular carcinoma (HepG2), and human neuroblastoma SHSY5Y cell lines was determined, and the results are presented in Table 6. The cytotoxic effect of different extracts on the tested cell lines was extract polarity dependent, where the cytotoxicity increased with decreasing the polarity of extracts. The EtOAc extract of the roots displayed a higher effect (cell viability = 29.30%) than that obtained from the aerial parts (cell viability 36.28%) towards the HepG2 cell line. Also, the same extract from both organs was highly toxic towards the HEK 293 cell (cell viability 11.72% and 10.73%). The cell viability of the malignant neuroblastoma SHSY5Y cells increased with increasing polarity of extracts in both organs, and the best cell viability percentage was obtained from the aqueous extract (114.19% and 110.64%). Overall, EtOAc extracts from both organs showed the strongest activity against HepG2 but were also cytotoxic to normal HEK293 cells. From the identified compounds in the present study, compounds like caffeoyl derivatives (Chen et al., 2014) and eupatorin (Patel, 2021) were found to possess remarkable anticancer activity against a panel of cancer cell lines. Kaempferol was shown to possess a significant antiproliferative effect on the HepG2 cell line (Wang et al., 2018). On the other hand, the three polar extracts of both organs induced a significant neuroprotective effect in the SH-SY5Y cells, with the highest effect observed in the aqueous extracts. Previous studies demonstrated that plant species like *Withania somnifera* (Wongtrakul et al., 2021), *Alternanthera sessilis, Eryngium foetidum*, and *Stephania japonica* (Hijam et al., 2024) displayed effective neuroprotective activity.

Cytotoxicity assays in this study were conducted at only one concentration. Although this preliminary method offers useful initial information on the cytotoxic potential of the samples tested, it poses a significant limitation, especially given the notable toxicity observed in normal cell lines. A comprehensive dose–response analysis, including IC_{50} values and selectivity indices, would provide a more precise evaluation of potency and therapeutic selectivity. Consequently, future research will expand these assays over multiple concentrations to more accurately determine the safety profile and potential therapeutic range of the studied extracts/compounds.

3.8 Computational Study

3.8.1 Molecular Docking

In this study, a total of 26 phytochemical compounds were identified as derivations of *Scorzonera coriacea*—including Kaempferol-3-*O*-glucoside, Catechin, Eupatorin, Dihydroxy-Trimethoxyflavone, Quercetin, Kaempferol, Eriodictyol-7-*O*-neohesperidoside, 5-Caffeoylquinic acid, Taxifolin, Isoquercitrin, Afzelin, 4-Hydroxycoumarin, Quercetin-3-*O*-rutinoside, Vanillin, Myricetin, Diosmetin, Malvidin-3-*O*-*β*-D-glucoside, 3,5-Dicaffeoylquinic acid, Diosmetin-7-*O*-glucoside, Apigenin-6-C-glucoside-8-C-arabinoside, 1,3-Dicaffeoylquinic acid, Hydroxycoumarin, Caffeic acid, Orientin, Umbelliferone, and Isoorientin—were subjected to molecular docking simulations using AutoDock Vina v1.1.2. These compounds were evaluated against a panel of 14 therapeutic targets, including classical catalytic enzymes: *α*-amylase, *α*-glucosidase, tyrosinase, AChE, BChE, and hepatocellular carcinoma (HepG2) cell–related proteins, such as AKT, BRPF1, CDK2, CDK4, Cyclin D1, MYC, PPARγ, PD-1, and TERT. Beyond the standard assay enzymes, all remaining targets were chosen for their relevance to HepG2 biology, covering proliferation/cell-cycle control, epigenetic/metabolic regulation (BRPF1, PPARγ), immune evasion (PD-1), and telomere maintenance (TERT). High-quality human PDB entries (ligand-bound where available) were prioritized to ensure active-site fidelity and enable redocking validation: AChE (7E3H), BChE (6EQP), Tyrosinase (6QXD), *α*-Amylase (2QV4), *α*-Glucosidase (7KBJ), AKT (4GV1), BRPF1 (5MWZ), CDK2 (6GUE), CDK4 (2W96), Cyclin D1 (2W99), MYC (1NKP), PD-1 (5N2F), TERT (5CQG), and PPARγ (1I7I). To improve focus, results are organized into predefined themes, with top-scoring pairs highlighted in the main text. Full rankings and one-line justifications with PDB IDs are provided in Table S2.

Among the 364 protein–ligand complexes that were generated, 62% exhibited binding energies below the $\Delta G \leq -7$ kcal/mol threshold, which is commonly accepted as indicative of strong affinity (Figure S17). These complexes were

http://doi.org/10.25135/rnp.2509.3633
Rec. Nat. Prod. 2026, 20(1):e25093633

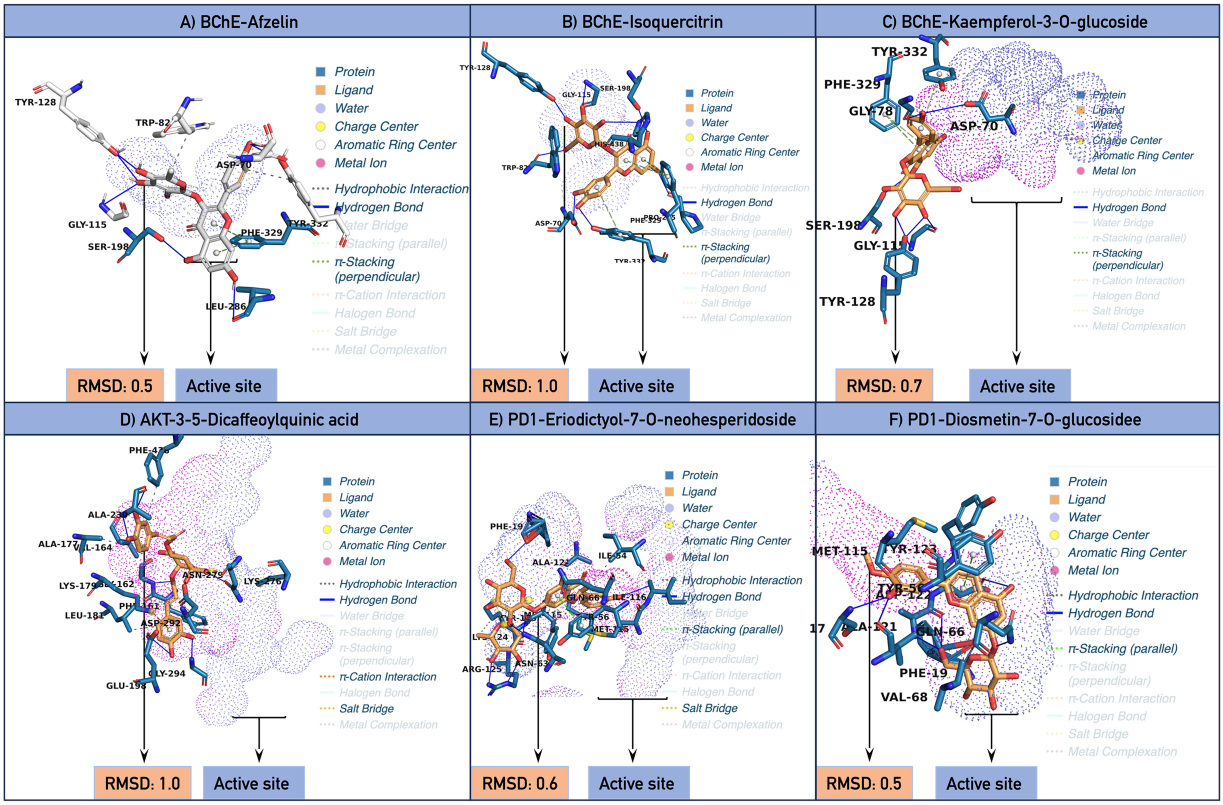

Figure 3. Representative docking poses of top-scoring ligand–target complexes within their active sites. A) BChE–Afzelin. B) BChE–Isoquercitrin. C) BChE–Kaempferol-3-O-glucoside. D) AKT–3,5-Dicaffeoylquinic acid. E) PD-1–Eriodictyol-7-O-neohesperidoside. F) PD-1–Diosmetin-7-O-glucoside

selected for further analysis. The reliability of the docking protocol was substantiated by the redocking results, which yielded RMSD values ranging from 0.0 to 48.5 Å. It is noteworthy that only 29 complexes exceeded 2 Å, while the majority exhibited high geometric alignment with their crystallographic reference poses. The overall binding affinities ranged from –1.4 kcal/mol (BChE–Isoorientin) to –10.7 kcal/mol (PD-1–Eriodictyol-7-O-neohesperidoside) (Figure 3E). With respect to enzymatic targets, five and nineteen compounds exceeded the affinity threshold for α-amylase and α-glucosidase, respectively. Eriodictyol-7-O-neohesperidoside showed the highest affinity for α-amylase (–10.1 kcal/mol), while diosmetin-7-O-glucoside was the most potent binder to α-glucosidase (–9.8 kcal/mol). These results suggest that both compounds may act as natural glycemic regulators. Furthermore, the consistent high-affinity interactions of Eriodictyol-7-O-neohesperidoside across multiple enzymes underscore its potential as a multi-target inhibitor. In the cholinergic enzyme group, 18 and 19 compounds exhibited strong binding to AChE and BChE, respectively. Myricetin (–9.9 kcal/mol), Afzelin, kaempferol-3-O-glucoside (–10.4 kcal/mol), and isoquercitrin (–10.6 kcal/mol) emerged as top candidates, indicating promising neuroprotective potential for use in neurodegenerative disorders (Figures 3A–3C). Interestingly, Isoquercitrin also showed notable binding to AKT, CDK2, and TERT, indicating a broader pharmacological profile capable of modulating multiple pathways simultaneously. In contrast, none of the tested compounds demonstrated strong binding to tyrosinase, with Kaempferol-3-O-glucoside reaching a maximum of –6.9 kcal/mol. This indicates the need for structural modification or derivatization to improve their efficacy against pigmentation-related targets. Among the cancer-associated proteins—specifically those overexpressed in HepG2 cells—numerous phytochemicals exhibited strong binding profiles. For AKT1, 3,5-Dicaffeoylquinic acid demonstrated the highest affinity (–10.4 kcal/mol), followed by diosmetin-7-O-glucoside and orientin (Figure 2D). CDK2 was most strongly inhibited by Orientin (–10.3 kcal/mol), with other top binders including 3,5-dicaffeoylquinic acid, eriodictyol-7-O-neohesperidoside, and isoquercitrin. These results point toward the potential of these compounds to interfere with key regulators of cell proliferation and survival in hepatocellular carcinoma. PD-1 was the most frequently and strongly targeted protein, with 25 compounds displaying binding energies below the –7 kcal/mol threshold. Eriodictyol-7-O-neohesperidoside again stood out with the most negative binding energy (–10.7 kcal/mol), followed closely by diosmetin-7-O-glucoside, quercetin, Taxifolin, and 3,5-Dicaffeoylquinic acid. These findings highlight the potential immunomodulatory and checkpoint inhibitory roles of these phytochemicals, particularly in immune-evasive tumors such as liver cancer (Figures 3E and 3F). For TERT, 21

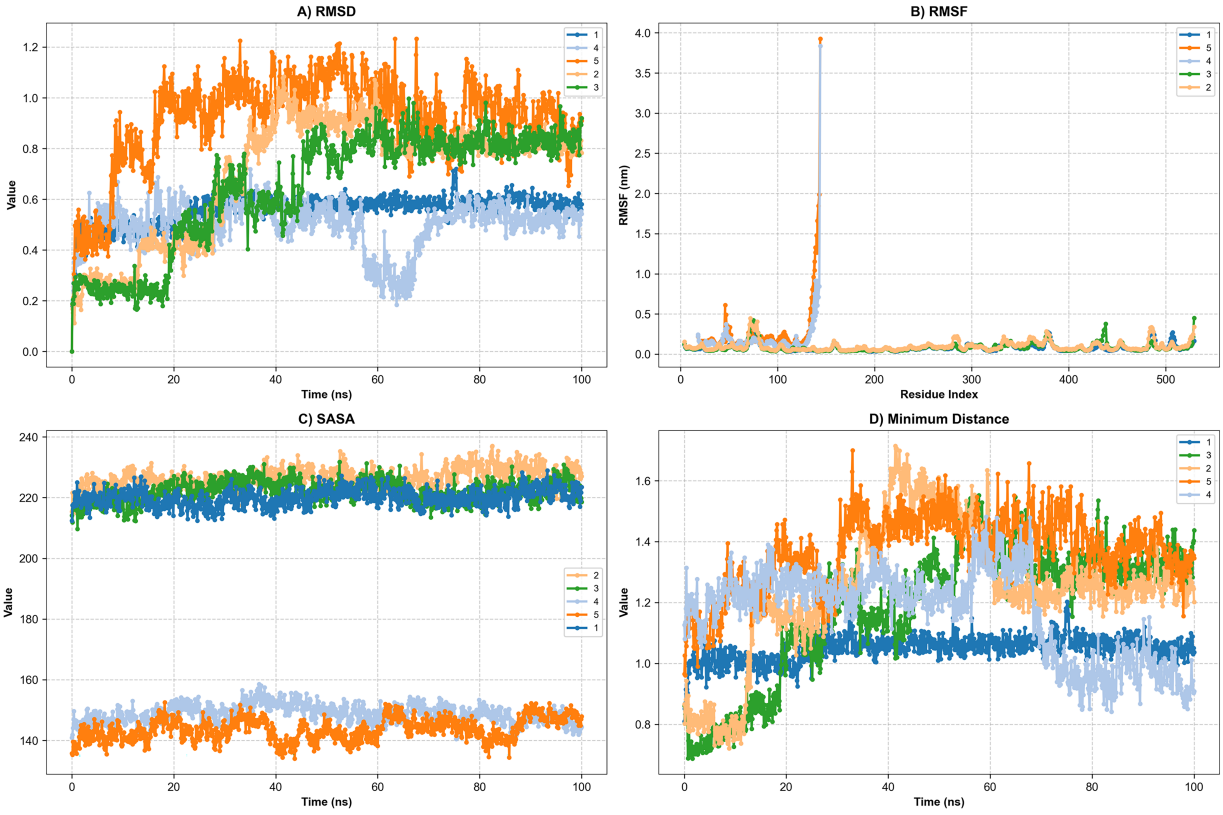

Figure 4. Representation of molecular dynamics simulations in graphical form; (A) RMSD. (B) RMSF. (C) SASA. (D) Minimum distance

compounds achieved high binding affinity, with kaempferol-3-O-glucoside and eriodictyol-7-O-neohesperidoside tying for the lowest ΔG value (–8.9 kcal/mol). Similarly, many compounds displayed notable affinity for BRPF1 and CDK4, suggesting their involvement in modulating epigenetic and cell-cycle–related mechanisms in hepatic tumor biology (Table S2).

Taken together, this comprehensive computational analysis demonstrates that flavonoids, phenolic acids, and glycosides derived from *S. coriacea* exhibit significant multi-target affinity, especially toward proteins overexpressed in hepatocellular carcinoma cells. Importantly, these computational predictions were in strong agreement with in vitro experimental results, further validating the biological relevance of the identified compounds. These results strongly support the hypothesis that the extract exerts antitumor activity not through a single mechanism but via a network of synergistic molecular interactions. Accordingly, the top-performing compounds identified here warrant further validation through in vitro and in vivo biological studies, as well as pharmacokinetic and toxicological profiling to determine their suitability as potential therapeutic candidates.

3.8.2 Molecular Dynamics Simulations

In this study, molecular dynamics (MD) simulations spanning 100 ns were conducted on five distinct ligand–target protein complexes to evaluate their structural and dynamic stability. The analyses encompassed a range of metrics, including root mean square deviation (RMSD), root mean square fluctuation (RMSF), solvent-accessible surface area (SASA), minimum binding distance, hydrogen bond count, and interaction duration. The systems that were examined were as follows: C1: BChE–Kaempferol-3-O-glucoside; C2: BChE–Isoquercitrin; C3: BChE–Afzelin; C4: BChE–Diosmetin-7-O-glucoside; and C5: PD-1–Eriodictyol-7-O-neohesperidoside. RMSD analysis revealed a substantial increase in complexes 2 and 3 throughout the simulation (C2 from 0.3 nM to 1.2 nM), indicating elevated conformational shifts and positional flexibility. On the other hand, complexes 1 and 4 showed minimal variation and nearly flat RMSD curves, indicating strong structural stability throughout the simulation. RMSF analysis revealed marked fluctuations in the 100–150 residue region, particularly in complexes 2 and 3, with complex 2 reaching around 4 nM, suggesting localized flexibility in that region. In contrast, the other complexes exhibited low RMSF values, especially near the binding sites, which implies greater structural rigidity (Figures 4A and 4B). SASA values remained consistent for complexes 3 and 5, averaging around 220–230 Å^2. Conversely, complex 2 had a smaller solvent-accessible surface area (approximately 140–160 Å^2), pointing to a more compact, yet potentially less stable, binding conformation (Figure 4C). The minimum binding distance showed a gradual increase over time in complexes 2, 3, and 5 (C2 from ≈0.8 nM to 1.5 nM), indicating loosening of ligand–protein interactions, while C1 maintained a largely stable distance, supporting sustained interaction fidelity (Figure 4D).

http://doi.org/10.25135/rnp.2509.3633
Rec. Nat. Prod. 2026, 20(1):e25093633

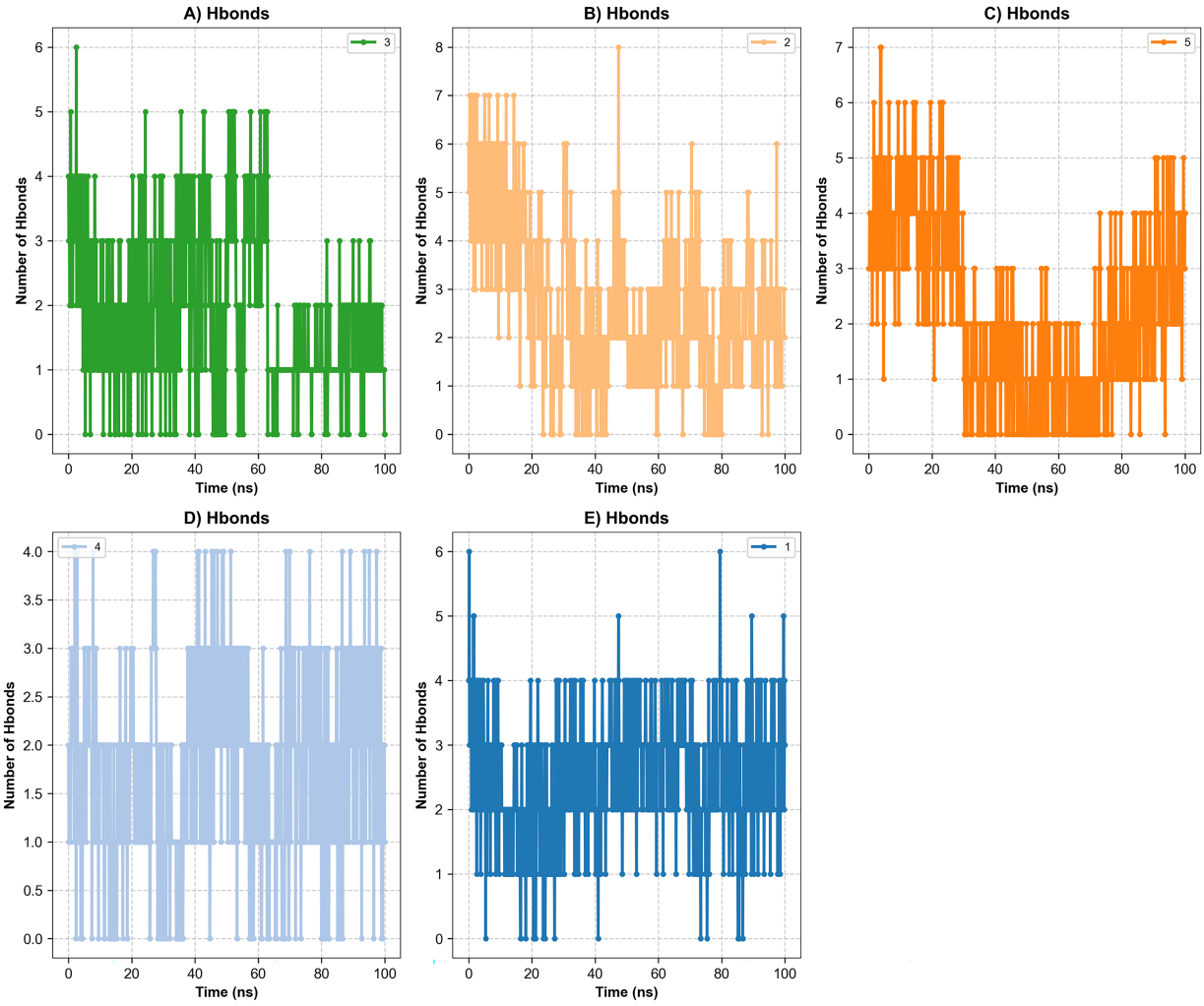

Figure 5. Time-dependent hydrogen bond analysis for each protein–ligand complex

Time-resolved hydrogen bond analysis corroborated these findings; the number of hydrogen bonds in complexes 2, 3, and 5 decreased significantly after the 40 ns mark (C2 from 5–6 to 0–2), reflecting weakening of polar interaction networks and reduced binding quality. Conversely, complex 4 exhibited stability in terms of both RMSD and binding distance, while demonstrating a gradual increase in hydrogen bonding. This finding suggests an adaptive binding pattern and a more securely anchored ligand configuration. Although all complexes remained within binding distance throughout the simulation, the nature and stability of these interactions varied significantly, particularly in terms of hydrogen bonding patterns and binding looseness observed over time. Consequently, complexes 1 and 4 were distinguished by their remarkable structural integrity, stable binding distances, and sustained or increasing hydrogen bond networks.

In contrast, complexes 2, 3, and 5 exhibited a comparatively less stable interaction profile, characterized by increased RMSD values, gradually widening binding distances, and a reduction in polar interactions (Figure 5). These results suggest that assessing the mere presence of binding is not sufficient; instead, the temporal stability and resilience of these interactions play a crucial role in determining therapeutic potential. Taken together, the findings indicate that C1 and C4 may serve as promising lead candidates for further drug development efforts, whereas C2, C3, and C5 could benefit from additional structural optimization and experimental follow-up to enhance their binding performance.

The current study highlighted the chemical composition, antioxidant, enzyme inhibitory, and cytotoxicity of *S. coriacea*. Both the aerial parts and roots were rich in total phenolic content, but the former accumulated higher total flavonoid content. Chemical analysis revealed the presence of organic acids, phenolic acids, flavonoids, coumarins, anthocyanins, terpenes, saponins, and fatty acids and their derivatives, with the aerial parts accumulating the highest number of compounds. Both organs displayed remarkable antioxidant activity, with the roots exhibiting the highest antiradical and ion-reducing capacity, while the aerial parts showed the highest chelating and total antioxidant activities. Complementary in silico analyses revealed 226 strong-binding protein–ligand complexes, with only tyrosinase showing poor affinity across all compounds. Molecular

dynamics simulations confirmed the stability of key complexes, particularly C1 and C4, while others showed weaker or unstable interactions over time. Also, both organs, mainly organic extracts, exerted significant enzyme-inhibitory activities. Cytotoxicity was extract polarity dependent, with the best effect towards HepG2 and HEK293 cell lines recorded from the least polar extract, while the aqueous extract induced the highest neuroprotective effect in the SH-SY5Y cells. These findings showed that *S. coriacea* could be a promising source of active ingredients. Future *in vivo* studies, isolation of bioactive compounds, and determination of their mechanism of action are recommended.

Author Contributions

Conceptualization: GA, SY, MVC, MJR, OAE, GZ; methodology: GA, MVC, MJR, EF, SHA, GZ, software: MVC, LC, EY; validation: SY, RT, GZ; formal analysis: LC, EY, GZ; investigation: GA, SY, MJR, EF, SHA, OAE, ANBS, GZ; resources: EY, GZ; data curation: GA, SY, MVC, RT, GZ; GZ writing–original draft preparation: GA, SY, MVC, GZ; writing–review and editing: EY, SHA, OAE, ANBS; visualization: MVC.; supervision: GZ, CLC; project administration: GZ.; funding acquisition: GZ.

Availability of Data and Materials

The authors declare that the data supporting the findings of this study are available within the paper and its Supplementary Information files. Should any raw data files be needed in another format they are available from the corresponding author upon reasonable request. Source data are provided with this paper.

Conflict of Interest

The authors declare they have no conflict of interest.

Supporting Information

Supporting information accompanies this paper on http://www.acgpubs.org/journal/records-of-natural-products.

ORCID

Gunes Ak: 0000-0002-9539-0763
Sakina Yagi: 0000-0002-9600-3526
Mehmet Veysi Cetiz: 0000-0002-2635-6553
Ramazan Tutus: 0000-0003-2297-7309
Maria J. Rodrigues: 0000-0001-8732-710X
Eliana Fernandes: 0000-0003-4083-8353
Luisa Custodio: 0000-0003-4338-7703
Evren Yildiztugay: 0000-0002-4675-2027
Shaza H. Aly: 0000-0003-2812-8340
Omayma A. Eldahshan: 0000-0002-0972-0560
Abdel Nasser B. Singab: 0000-0001-7445-963X
Gokhan Zengin: 0000-0001-6548-7823

References

Abdelazim, E. B., Abed, T., Goher, S. S., Alya, S. H., El-Nashar, H. A., El-Moslamy, S. H., El-Fakharany, E. M., Abdul-Baki, E. A., Shakweer, M. M., & Eissa, N. G. (2024). In vitro and in vivo studies of *Syzygium cumini*-loaded electrospun PLGA/PMMA/collagen nanofibers for accelerating topical wound healing. *RSC Advances*, *14*(1), 101–117. DOI: 10.1039/d3ra06355k.

Abdl Aziz, F. T., Temraz, A. S. & Hassan, M. A. (2024). Metabolites profiling by LC-ESI-MS/MS technique and in-vitro antioxidant activity of *Bauhinia madagascariensis* Desv. and Bauhinia purpurea L. aerial parts cultivated in Egypt: a comparative study. *Azhar International Journal of Pharmaceutical and Medical Sciences*, *4*(1), 169–188. DOI: 10.21608/aijpms.2023.212409.1215.

AbouZeid, E. M., Afifi, A. H., Salama, A., Hussein, R. A., Youssef, F. S., El-Ahmady, S. H. & Ammar, N. M. (2022). Comprehensive metabolite profiling of *Phoenix rupicola* pulp and seeds using UPLC-ESI-MS/MS and evaluation of their estrogenic activity in ovariectomized rat model. *Food Research International*, *157*(1), 111308. DOI: 10.1016/j.foodres.2022.111308.

Ajebli, M., Amssayef, A., Sabiri, M., Radi, F. Z., Bouhlali, E. D. T. & Eddouks, M. (2025). *Scorzonera undulata*: traditional applications, phytochemical analysis, and biological and pharmacological attributes. *Plants (Basel)*, *14*(11), 1606. DOI: 10.3390/plants14111606.

Ak, G., Dall'Acqua, S., Sut, S., Ferrarese, I., Yıldıztugay, E., Mahomoodally, M. F., Sinan, K. I., Sadeer, N. B., Rengasamy, K. R. & Zengin, G. (2020a). Chemical characterization and bio-pharmaceutical abilities of five different solvent extracts from aerial parts and roots of *Scorzonera hispanic*a L. *South African Journal of Botany*, *133*(81), 212–221. DOI: 10.1016/j.sajb.2020.08.003.

Ak, G., Dall'Acqua, S., Sut, S., Ferrarese, I., Yıldıztugay, E., Mahomoodally, M. F., Sinan, K. I., Sadeer, N. B., Rengasamy, K. R. R. & Zengin, G. (2020b). Chemical characterization and bio-pharmaceutical abilities of five different solvent extracts from aerial parts and roots of *Scorzonera hispanica* L. *South African Journal of Botany*, *133*(81), 212–221. DOI: 10.1016/j.sajb.2020.08.003.

Aly, S. H., Elissawy, A. M., Mahmoud, A. M., El-Tokhy, F. S.e, Mageed, S. S. A., Almahli, H., Al-Rashood, S. T., Binjubair, F. A., Hassab, M. A. E. & Eldehna, W. M. (2023). Synergistic effect of *Sophora japonica* and *Glycyrrhiza glabra* flavonoid-rich fractions on wound healing: in vivo and molecular docking studies. *Molecules*, *28*(7), 2994. DOI: 10.3390/molecules28072994.

Aly, S. H., Elissawy, A. M., El Hassab, M. A., Majrashi, T. A., Hassan, F. E., Elkaeed, E. B., Eldehna, W. M. & Singab, A. N. B. (2024a). Comparative metabolic study of the chloroform fraction of three *Cystoseira* species based on UPLC/ESI/MS analysis and biological activities. *Journal of Enzyme Inhibition and Medicinal Chemistry*, *39*(1), 2292482.

Aly, S. H., Mahmoud, A. M., Abdel Mageed, S. S., Khaleel, E. F., Badi, R. M., Elkaeed, E. B., Rasheed, R. A., El Hassab, M. A. & Eldehna, W. M. (2024b). Exploring the phytochemicals, antioxidant properties, and hepatoprotective potential of *Moricandia sinaica* leaves against paracetamol-induced toxicity: Biological evaluations and in Silico insights. *PLoS One*, *19*(10), e0307901. DOI: 10.1371/journal.pone.0307901.

Angeles Flores, G., Cusumano, G., Zengin, G., Cetiz, M. V., Uba, A. I., Senkardes, I., Koyuncu, I., Yuksekdag, O., Kalyniukova, A. & Emiliani, C. (2024). Using in vitro and in silico analysis to investigate the chemical profile and biological properties

of *Polygonum istanbulicum* extracts. *Plants*, *13*(23), 3421. DOI: 10.3390/plants13233421.

Atasagun, B., Uysal, A., Fathallah, N., Eldahshan, O., Singab, A. N., Cetiz, M. V. & Zengin, G. (2025). Exploring the utility of *Prunus mahaleb* extracts as a source of natural bioactive compounds for functional applications. *Food Science & Nutrition*, *13*(4), e70121.

Ayoub, I. M., Korinek, M., El-Shazly, M., Wetterauer, B., El-Beshbishy, H. A., Hwang, T.-L., Chen, B.-H., Chang, F.-R., Wink, M. & Singab, A. N. B. (2021). Anti-allergic, anti-inflammatory, and anti-hyperglycemic activity of *Chasmanthe aethiopica* leaf extract and its profiling using LC/MS and GLC/MS. *Plants*, *10*(6), 1118. DOI: 10.3390/plants10061118.

Ayromlou, A., Masoudi, S. & Mirzaie, A. (2020). Chemical composition, antioxidant, antibacterial, and anticancer activities of *Scorzonera calyculata* Boiss. and *Centaurea irritans* Wagenitz. Extracts, endemic to iran. *Journal of Reports in Pharmaceutical Sciences*, *9*(1), 118–127.

Baloglu, M. C., Ozer, L. Y., Pirci, B., Altunoglu, Y. C., Soomro, S. I., Zengin, G., Cetiz, M. V., Carradori, S., Cziáky, Z. & Jekő, J. (2025). Decoding chemical profiles, biological functions, and medicinal properties of *Liquidambar orientalis* extracts through molecular modeling and bioinformatic methods. *Food Frontiers*, *6*, 1376–1408.

Benayad, Z., Gómez-Cordovés, C. & Es-Safi, N. E. (2014). Characterization of flavonoid glycosides from fenugreek (*Trigonella foenum-graecum*) crude seeds by HPLC-DAD–ESI/MS analysis. *International Journal of Molecular Sciences*, *15*(11), 20668–20685. DOI: 10.3390/ijms151120668.

Bursal, E., Taslimi, P., Gören, A. C. & Gülçin, İ. (2020). Assessments of anticholinergic, antidiabetic, antioxidant activities and phenolic content of *Stachys annua*. *Biocatalysis and Agricultural Biotechnology*, *28*(3), 101711. DOI: 10.1016/j.bcab.2020.101711.

Cetiz, M. V., Ahmed, S., Zengin, G., Sinan, K. I., Emre, G., Dolina, K., Kalyniukova, A., Uba, A. I., Koyuncu, I. & Yuksekdag, O. (2025). Bioinformatic and experimental approaches to uncover the bio-potential of *Mercurialis annua* extracts based on chemical constituents. *Journal of Molecular Liquids*, *427*, 127390. DOI: 10.1016/j.molliq.2025.127390.

Cetiz, M. V., Isah, M., Ak, G., Bakar, K., Himidi, A. A., Mohamed, A., Glamočlija, J., Nikolić, F., Gašic, U. & Cespedes-Acuna, C. L. (2024). Exploring of chemical profile and biological activities of three *Ocimum* species from Comoros Islands: A combination of in vitro and in silico insights. *Cell Biochemistry and Function*, *42*(7), e70000. DOI: 10.1002/cbf.70000.

Chakraborty, A., Chaudhury, R., Dutta, S., Basak, M., Dey, S., Schäffner, A. R. & Das, M. (2022). Role of metabolites in flower development and discovery of compounds controlling flowering time. *Plant Physiology and Biochemistry*, *190*, 109–118.

Chen, H.-z., Chen, Y.-b., Lv, Y.-p., Zeng, F., Zhang, J., Zhou, Y.-l., Li, H.-b., Chen, L.-f., Zhou, B.-j. & Gao, J.-r. (2014). Synthesis and antitumor activity of feruloyl and caffeoyl derivatives. *Bioorganic & Medicinal Chemistry Letters*, *24*(18), 4367–4371.

Chiavaroli, A., Libero, M. L., Di Simone, S. C., Acquaviva, A., Nilofar, Recinella, L., Leone, S., Brunetti, L., Cicia, D., Izzo, A. A., Orlando, G., Zengin, G., Uba, A. I., Cakilcioğlu, U., Mukemre, M., Elkiran, O., Menghini, L. & Ferrante, C. (2023). Adding new scientific evidences on the pharmaceutical properties of *Pelargonium quercetorum* Agnew extracts by using in vitro and in silico approaches. *Plants*, *12*(5), 1132. DOI: 10.3390/plants12051132.

Cusumano, G., Flores, G. A., Cetiz, M. V., Kurt, U., Ak, G., Saka, E., Aly, S. H., Eldahshan, O. A., Singab, A. N. & Zengin, G. (2024). Small steps to the big picture for health-promoting applications through the use of Chickweed (*Stellaria media*): in vitro, in dilico, and pharmacological network approaches. *Food Science & Nutrition*, *12*(11), 9295–9313. DOI: 10.1002/fsn3.4505.

Dall'Acqua, S., Ak, G., Sut, S., Zengin, G., Yıldıztugay, E., Mahomoodally, M. F., Sinan, K. I. & Lobine, D. (2020a). Comprehensive bioactivity and chemical characterization of the endemic plant *Scorzonera hieraciifolia* Hayek extracts: a promising source of bioactive compounds. *Food Research International*, *137*(1), 109371. DOI: 10.1016/j.foodres.2020.109371.

Dall'Acqua, S., Ak, G., Sut, S., Ferrarese, I., Zengin, G., Yıldıztugay, E., Mahomoodally, M. F., Sinan, K. I. & Lobine, D. (2020b). Phenolics from Scorzonera tomentosa L.: exploring the potential use in industrial applications via an integrated approach. *Industrial Crops and Products*, *154*(10), 112751. DOI: 10.1016/j.indcrop.2020.112751.

Deng, S.-P., Yang, Y.-L., Cheng, X.-X., Li, W.-R. & Cai, J.-Y. (2019). Synthesis, spectroscopic study and radical scavenging activity of kaempferol derivatives: Enhanced water solubility and antioxidant activity. *International Journal of Molecular Sciences*, *20*(4), 975.

Dileep, K. V., Ihara, K., Mishima-Tsumagari, C., Kukimoto-Niino, M., Yonemochi, M., Hanada, K., Shirouzu, M. & Zhang, K. Y. J. (2022). Crystal structure of human acetylcholinesterase in complex with tacrine: implications for drug discovery. *International Journal of Biological Macromolecules*, *210*, 172–181.

Duran, A., Dogan, B., Hamzaoglu, E. & Aksoy, A. (2011). *Scorzonera coriacea* A. Duran & Aksoy (Asteraceae, Cichorieae), a new species from South Anatolia, Turkey. *Candollea*, *66*(2), 353–359.

El Kamari, F., El Omari, H., El-Mouhdi, K., Chlouchi, A., Harmouzi, A., Lhilali, I., El Amrani, J., Zahouani, C., Hajji, Z. & Ousaaid, D. (2024). Effects of different solvents on the total phenol content, total flavonoid content, antioxidant, and antifungal activities of *Micromeria graeca* L. from Middle Atlas of Morocco. *Biochemistry Research International*, *2024*(1), 9027997. DOI: 10.1155/2024/9027997.

El-Nashar, H. A., Zengin, G., Tarek, A. & Eldahshan, O. A. (2025). Comparative metabolic profiling of *Cordia myxa* leaves and fruits based on UPLC-ESI/MS-MS analysis and investigation of antioxidant activities and enzyme inhibitory properties. *Scientific Reports*, *15*(1), 19296. DOI: 10.1038/s41598-025-04015-2.

Ercan, S., Kurtul, E., Yilmaz, Ö. & Acıkara, Ö.B. (2024). Validated Hplc method to analyze phytochemical structure of *Scorzonera* Species Grown In Türkiye. *Journal of Faculty of Pharmacy of Ankara University*, *48*(3), 32.

Erez, E., Babakr, S. H., Mükemre, M. & Dalar, A. (2022). The phenolic profile and biological activities of common *Scorzonera* species from Eastern Anatolia [The phenolic profile and biological activities of common Scorzonera species from Eastern Anatolia]. *International Journal of Secondary Metabolite*, *9*(4), 538–550.

Erik, İ., Yaylı, N., Coşkunçelebi, K., Makbul, S. & Karaoğlu, Ş. A. (2021). Three new dihydroisocoumarin glycosides with antimicrobial activities from *Scorzonera aucheriana*. *Phytochemistry Letters*, *43*(5), 45–52. DOI: 10.1016/j.phytol.2021.02.010.

Fan, M., Zhang, G., Hu, X., Xu, X. & Gong, D. (2017). Quercetin as a tyrosinase inhibitor: inhibitory activity, conformational change and mechanism. *Food Research International*, *100*, 226–233.

Farag, M. A., Abdelwareth, A., Zayed, A., Eissa, T. F., Dokalahy, E., Frolov, A. & Wessjohann, L. A. (2022). A comparative metabolomics approach for Egyptian mango fruits classification based on UV and UPLC/MS and in relation to its antioxidant effect. *Foods*, *11*(14), 2127. DOI: 10.3390/foods11142127.

Farag, M. A., Gad, H. A., Heiss, A. G. & Wessjohann, L. A. (2014). Metabolomics driven analysis of six *Nigella*

species seeds via UPLC-qTOF-MS and GC-MS coupled to chemometrics. *Food Chemistry*, *151*(2), 333–342. DOI: 10.1016/j.foodchem.2013.11.032.

Farag, M. A., El Fishawy, A. M., El-Toumy, S. A., Amer, K. F., Mansour, A. M. & Taha, H. E. (2016a). Antihepatotoxic effect and metabolite profiling of *Panicum turgidum* extract via UPLC-qTOF-MS. *Pharmacognosy magazine*, *12*(Suppl 4), S446.

Farag, M. A., Otify, A., Porzel, A., Michel, C. G., Elsayed, A. & Wessjohann, L. A. (2016b). Comparative metabolite profiling and fingerprinting of genus *Passiflora* leaves using a multiplex approach of UPLC-MS and NMR analyzed by chemometric tools. *Analytical and Bioanalytical Chemistry*, *408*(12), 3125–3143. DOI: 10.1007/s00216-016-9376-4.

Farag, M. A., Sharaf Eldin, M. G., Kassem, H. & Abou el Fetouh, M. (2013). Metabolome classification of *Brassica napus* L. organs via UPLC-QTOF–PDA-MS and their anti-oxidant potential. *Phytochemical Analysis*, *24*(3), 277–287. DOI: 10.1002/pca.2408.

Gladis, C., Ramana, K. V., Subramanyam, C., Rao, H., Rao, V. M., Satyanarayana, G. & Malar, R. (2025). ZnO catalyzed microwave synthesis of novel α-Nano diabetic potential via molecular docking,-aminophosphonates: anti amylase inhibition studies. *Organic Communications*. DOI: 10.25135/acg.oc.187.2501.3413.

Goher, S. S., Aly, S. H., Abu-Serie, M. M., El-Moslamy, S. H., Allam, A. A., Diab, N. H., Hassanein, K. M., Eissa, R. A., Eissa, N. G. & Elsabahy, M. (2024). Electrospun Tamarindus indica-loaded antimicrobial PMMA/cellulose acetate/PEO nanofibrous scaffolds for accelerated wound healing: in-vitro and in-vivo assessments. *International Journal of Biological Macromolecules*, *258*(1), 128793. DOI: 10.1016/j.ijbiomac.2023.128793.

Gong, Y., Shi, Z.-N., Yu, J., He, X.-F., Meng, X.-H., Wu, Q.-X. & Zhu, Y. (2024). The genus *Scorzonera* L.(Asteraceae): a comprehensive review on traditional uses, phytochemistry, pharmacology, toxicology, chemotaxonomy, and other applications. *Journal of Ethnopharmacology*, *320*(19), 116787. DOI: 10.1016/j.jep.2023.116787.

Goufo, P., Singh, R. K. & Cortez, I. (2020). A reference list of phenolic compounds (including stilbenes) in grapevine (*Vitis vinifera* L.) roots, woods, canes, stems, and leaves. *Antioxidants*, *9*(5), 398. DOI: 10.3390/antiox9050398.

Granica, S., Lohwasser, U., Jöhrer, K. & Zidorn, C. (2015). Qualitative and quantitative analyses of secondary metabolites in aerial and subaerial of *Scorzonera hispanica* L.(black salsify). *Food Chemistry*, *173*, 321–331. DOI: 10.1016/j.foodchem.2014.10.006.

Grochowski, D. M., Uysal, S., Aktumsek, A., Granica, S., Zengin, G., Ceylan, R., Locatelli, M. & Tomczyk, M. (2017). In vitro enzyme inhibitory properties, antioxidant activities, and phytochemical profile of *Potentilla thuringiaca*. *Phytochemistry Letters*, *20*, 365–372. DOI: 10.1016/j.phytol.2017.03.005.

Gurumayum, S., Bharadwaj, S., Sheikh, Y., Barge, S. R., Saikia, K., Swargiary, D., Ahmed, S. A., Thakur, D. & Borah, J. C. (2023). Taxifolin-3-O-glucoside from *Osbeckia nepalensis* Hook. mediates antihyperglycemic activity in CC1 hepatocytes and in diabetic Wistar rats via regulating AMPK/G6Pase/PEPCK signaling axis. *Journal of Ethnopharmacology*, *303*(2), 115936. DOI: 10.1016/j.jep.2022.115936.

Günal-Köroğlu, D., Catalkaya, G., Yusufoğlu, B., Kezer, G., Esatbeyoglu, T., Abd El-Aty, A. & Capanoglu, E. (2025). Quercetin: potential antidiabetic effects through enzyme inhibition and starch digestibility. *Food Safety and Health*, *3*(1), 9–22.

Han, H., Yilmaz, H. & Gulcin, I. (2018). Antioxidant activity of flaxseed (Linum usitatissimum L.) shell and analysis of its polyphenol contents by LC-MS/MS. *Records of Natural Products*, *12*, 397–402.

Han, Z., Wang, L., Sun, P., Huang, M., Yu, F., Liu, J., Wu, Y., He, P., Tu, Y. & Li, B. (2024). Quinic acid as an inhibitor of α-glucosidase activity, nonenzymatic glycosylation, and glucose transport in Caco-2 cells. *Food Frontiers*, *5*(6), 2545–2555. DOI: 10.1002/fft2.486.

Harkati, B., Akkal, S., Bayat, C., Laouer, H. & Franca, M. D. (2010). Secondary metabolites from *Scorzonera undulata* ssp. deliciosa (Guss.) Maire (Asteracae) and their antioxidant activities. *Records of Natural Products*, *4*(3), 171.

Hijam, A. C., Tongbram, Y. C., Nongthombam, P. D., Meitei, H. N., Koijam, A. S., Rajashekar, Y. & Haobam, R. (2024). Neuroprotective potential of traditionally used medicinal plants of Manipur against rotenone-induced neurotoxicity in SH-SY5Y neuroblastoma cells. *Journal of Ethnopharmacology*, *330*(4), 118197. DOI: 10.1016/j.jep.2024.118197.

Idoudi, S., Othman, K. B., Bouajila, J., Tourrette, A., Romdhane, M. & Elfalleh, W. (2023). Influence of extraction techniques and solvents on the antioxidant and biological potential of different parts of *Scorzonera undulata*. *Life*, *13*(4), 904. DOI: 10.3390/life13040904.

Islam, S., Adam, Z. & Akanda, J. H. (2024). Quinic and caffeic acids derivatives: affecting antioxidant capacities and phenolics contents of certain therapeutic and specialty crops employing water and ethanolic extracts. *Food Chemistry Advances*, *4*(13), 100693. DOI: 10.1016/j.focha.2024.100693.

Jo, S., Kim, T., Iyer, V. G. & Im, W. (2008). CHARMM-GUI: a web-based graphical user interface for CHARMM. *Journal of Computational Chemistry*, *29*(11), 1859–1865. DOI: 10.1002/jcc.20945.

Karta, S., Çarıkçı, S., Dirmenci, T., Kılıç, T. & Goren, A. C. (2025). Determination of secondary metabolites of two *Satureja* species by LC-HRMS and evaluation of their antioxidant and anti-Alzheimer capacity. *Journal of Chemical Metrology*, *19*, 82–93.

Khattab, O. M., El-Kersh, D. M., Khalifa, S. A., Yosri, N., El-Seedi, H. R. & Farag, M. A. (2023). Comparative MS-and NMR-based metabolome mapping of Egyptian red and white squill bulbs F. Liliaceae and in relation to their cytotoxic effect. *Plants*, *12*(11), 2078. DOI: 10.3390/plants12112078.

Kınoğlu, B. K., Gülçin, İ. & Gören, A. C. (2024). Quantification of secondary metabolites of *Satureja pilosa* (Lamiaceae) by LC-HRMS and evaluation of antioxidant and cholinergic activities. *Records of Natural Products*, *18(6)*, 674–686.

Korpayev, S., Zengin, G., Ak, G., Glamočlija, J., Soković, M., Aničić, N., Gašić, U., Stojković, D., Agamyradov, M. & Cetiz, M. V. (2025). Integration of in vitro and in silico results from chemical and biological assays of *Rheum turkestanicum* and *Calendula officinalis* flower extracts. *Food Science & Nutrition*, *13*(1), e4663. DOI: 10.1002/fsn3.4663.

Lesjak, M., Beara, I., Simin, N., Pintać, D., Majkić, T., Bekvalac, K., Orčić, D. & Mimica-Dukić, N. (2018). Antioxidant and anti-inflammatory activities of quercetin and its derivatives. *Journal of Functional Foods*, *40*, 68–75.

Liao, Y., Mai, X., Wu, X., Hu, X., Luo, X. & Zhang, G. (2022). Exploring the inhibition of quercetin on acetylcholinesterase by multispectroscopic and in silico approaches and evaluation of its neuroprotective effects on PC12 cells. *Molecules*, *27*(22), 7971.

Lin, Z., Cheng, X. & Zheng, H. (2023). Umbelliferon: a review of its pharmacology, toxicity and pharmacokinetics. *Inflammopharmacology*, *31*(4), 1731–1750.

Llorent-Martínez, E. J., Yagi, S., Zengin, G., Cetiz, M. V., Uba, A. I., Yuksekdag, O., Akgul, B. H., Yildiztugay, E. & Koyuncu, I. (2025). Characterization of the chemical profiles and biological

activities of *Thesium bertramii* Azn. Extracts using a combination of in vitro, in silico, and network pharmacology methods. *Fitoterapia*, *180*, 106329.

Magdy, M., Elosaily, A. H., Mohsen, E., EL Hefnawy, H. M. (2024). Chemical profile, antioxidant and anti-Alzheimer activity of leaves and flowers of *Markhamia lutea* cultivated in Egypt: in vitro and in silico studies. *Future Journal of Pharmaceutical Sciences*, *10*(1), 103. DOI: 10.1186/s43094-024-00679-1.

Mahdi, B., Azmi, M. N., Phongphane, L., Abd Ghani, M. S., Bakar, M. H. A., Omar, M. T. C., Mikhaylov, A. A. & Supratman, U. (2024). Synthesis of ortho-carboxamidostilbene analogues and their antidiabetic activity through in vitro and in silico approaches. *Organic Communications*, *17*(1), 22.

Maier, J. A., Martinez, C., Kasavajhala, K., Wickstrom, L., Hauser, K. E. & Simmerling, C. (2015). ff14SB: improving the accuracy of protein side chain and backbone parameters from ff99SB. *Journal of Chemical Theory and Computation*, *11*(8), 3696–3713.

Mallikarjunaswamy, A. M., Gouthami, K., Maity, S., Reddy, V. D. & Basavegowda, L. (2024). Synthesis, characterization, antioxidant, in silico-based virtual screening and anti-cancer potential of substituted 2-(4-acetyl-5-methyl-1h-1, 2, 3-triazol-1-yl)-n-phenylacetamide derivatives. *Organic Communications*, *17*(4), 240.

Nilofar, N., Zengin, G., Acar, M., Bouyayha, A., Youssra, A., Eldahshan, O., Fayez, S. & Fahmy, N. (2024). Assessing the chemical composition, antioxidant and enzyme inhibitory effects of *Pentapleura subulifera* and *Cyclotrichium glabrescens* extracts. *Chemistry & Biodiversity*, *21*(2), e202301651. DOI: 10.1002/cbdv.202301651.

Özer, Z., Çarıkçı, S., Kılıç, T., Selvi, S. & Gören, A. C. (2024). Determination of the effect of different drying methods on secondary metabolites of Lavandula pedunculata (Mill.) Cav. subsp. cariensis (Boiss.) Upson & S. Andrews by LC-HRMS. *Journal of Chemical Metrology*, *18*(2). DOI: 10.25135/jcm.119.2411.3382.

Özcan Aykutlu, A., Makbul, S., Coşkunçelebi, K. & Seyis, F. (2025). Secondary volatile metabolite composition in scorzonera pseudolanata grossh. Plant parts. *Plants.*, *14*(11), 1624. DOI: 10.3390/plants14111624.

Paraschos, S., Magiatis, P., Kalpoutzakis, E., Harvala, C. & Skaltsounis, A.-L. (2001). Three new dihydroisocoumarins from the Greek endemic species *Scorzonera cretica*. *Journal of Natural Products*, *64*(12), 1585–1587.

Patel, D. K. (2021). Medicinal importance of flavonoid "Eupatorin" in the health sectors: therapeutic benefit and pharmacological activities through scientific data analysis. *Current Chinese Science*, *1*(6), 629–638. DOI: 10.2174/2210298101666210804141644.

Peng, X., Zhang, G., Liao, Y. & Gong, D. (2016). Inhibitory kinetics and mechanism of kaempferol on α-glucosidase. *Food Chemistry*, *190*, 207–215.

Praveena, R., Sadasivam, K., Deepha, V. & Sivakumar, R. (2014). Antioxidant potential of orientin: a combined experimental and DFT approach. *Journal of Molecular Structure*, *1061*, 114–123.

Rodrigues, M. J., Neves, V., Martins, A., Rauter, A. P., Neng, N. R., Nogueira, J. M., Varela, J., Barreira, L. & Custódio, L. (2016). In vitro antioxidant and anti-inflammatory properties of *Limonium algarvense* flowers' infusions and decoctions: a comparison with green tea (*Camellia sinensis*). *Food Chemistry*, *200*, 322–329. DOI: 10.1016/j.foodchem.2016.01.048.

Rosenberry, T. L., Brazzolotto, X., Macdonald, I. R., Wandhammer, M., Trovaslet-Leroy, M., Darvesh, S. & Nachon, F. (2017). Comparison of the binding of reversible inhibitors to human butyrylcholinesterase and acetylcholinesterase: a crystallographic, kinetic and calorimetric study. *Molecules*, *22*(12). DOI: 10.3390/molecules22122098.

Şahin, H., Demir, S., Boğa, M., Sarı, A., Makbul, S. & Gültepe, M. (2023). Comparative phytochemical and bioactivity studies on two related *Scorzonera* L. species: A chemotaxonomic contribution. *Biochemical Systematics and Ecology*, *111*(26), 104743. DOI: 10.1016/j.bse.2023.104743.

Şahin, H., Sarı, A., Özsoy, N. & Çelik, B.Ö. (2020a). Phenolic compounds and bioactivity of *Scorzonera pygmaea* Sibth. & Sm. aerial parts: In vitro antioxidant, anti-inflammatory and antimicrobial activities. *İstanbul Journal of Pharmacy*, *50*(3), 294–299.

Şahin, H., Sarı, A., Özsoy, N., Özbek Çelik, B. & Koyuncu, O. (2020b). Two new phenolic compounds and some biological activities of *Scorzonera pygmaea* Sibth. & Sm. subaerial parts. *Natural Product Research*, *34*(5), 621–628.

Sarıaltın, S. Y. & Acıkara, Ö.B. (2022). Assessment of correlation analysis, phytochemical profile, and biological activities of endemic *Scorzonera* species from Turkey. *Chemistry & Biodiversity*, *19*(10), e202200007. DOI: 10.1002/cbdv.202200007.

Sarimahmut, M. (2023). Investigation of the dual role of *Scorzonera pygmaea*: Cytotoxic activity and antioxidant potential. *Journal of Food Processing and Preservation*, *2023*(1), 2663247. DOI: 10.1155/2023/2663247.

Seyis, F., Makbul, S. & Coşkunçelebi, K. (2025). Chemical composition in various plant sections of *Scorzonera kotschyi* Bois. (Asteraceae). *Flavour and Fragrance Journal*, *50*(34), 239. DOI: 10.1002/ffj.70029.

Shang Jin, S. J., Xin Yan, X. Y., Feng HongXia, F. H. & Wang ZhenYu, W. Z. (2011). Comparative study of Kaempferol and Arbutin in action of melanocytes. *Chinese Journal of Dermatovenereology*, *25*, 185–187.

Shi, W., Zhang, G., Liao, Y., Fei, X., Gong, D. & Hu, X. (2023). Anti-acetylcholinesterase mechanism of kaempferol and its synergistic effect with galanthamine hydrobromide. *Food Bioscience*, *56*, 103174.

Tajner-Czopek, A., Gertchen, M., Rytel, E., Kita, A., Kucharska, A. Z. & Sokół-Łętowska, A. (2020). Study of antioxidant activity of some medicinal plants having high content of caffeic acid derivatives. *Antioxidants*, *9*(5), 412. DOI: 10.3390/antiox9050412.

Temiz, M. (2021). Antioxidant and antihyperglycemic activities of *Scorzonera cinerea* radical leaves in streptozocin-induced diabetic rats. *Acta Pharmaceutica*, *71*(4), 603–617. DOI: 10.2478/acph-2021-0045.

Wang, J., Fang, X., Ge, L., Cao, F., Zhao, L., Wang, Z. & Xiao, W. (2018). Antitumor, antioxidant and anti-inflammatory activities of kaempferol and its corresponding glycosides and the enzymatic preparation of kaempferol. *PLoS One*, *13*(5), e0197563.

Wongtrakul, J., Thongtan, T., Kumrapich, B., Saisawang, C. & Ketterman, A. J. (2021). Neuroprotective effects of *Withania somnifera* in the SH-SY5Y Parkinson cell model. *Heliyon*, *7*(10). DOI: 10.1016/j.heliyon.2021.e08172.

Xie, Y., Guo, Q.-S. & Wang, G.-S. (2016). Preparative separation and purification of the total flavonoids in Scorzonera austriaca with macroporous resins. *Molecules*, *21*(6), 768. DOI: 10.3390/molecules21060768.

Yagi, S., Cetiz, M. V., Zengin, G., Bakar, K., Himidi, A. A., Mohamed, A., Skorić, M., Glamočlija, J. & Gašić, U. (2025). Novel natural candidates for replacing synthetic additives in

nutraceutical and pharmaceutical areas: two *Senna* species (*S. alata* (L.) Roxb. and *S. occidentalis* (L.) Link). *Food Science & Nutrition*, *13*(1), e4705.

Yildirim, M. A., Sevinc, B., Paydas, S., Karaselek, M. A., Duran, T., Kuccukturk, S., Vatansev, H., Cetiz, M. V., Caprioli, G. & Acquaticci, L. (2025). Exploring the anticancer potential of Dianthus orientalis in pancreatic cancer: A molecular and cellular study. *Food Bioscience*, *66*, 106183.

Zengin, G., Fahmy, N. M., Sinan, K. I., Uba, A. I., Bouyahya, A., Lorenzo, J. M., Yildiztugay, E., Eldahshan, O. A. & Fayez, S. (2022). Differential metabolomic fingerprinting of the crude extracts of three Asteraceae species with assessment of their in vitro antioxidant and enzyme-inhibitory activities supported by in silico investigations. *Processes*, *10*(10), 1911. DOI: 10.3390/pr10101911.

Zengin, G., Nithiyanantham, S., Locatelli, M., Ceylan, R., Uysal, S., Aktumsek, A., Selvi, P. K. & Maskovic, P. (2016). Screening of in vitro antioxidant and enzyme inhibitory activities of different extracts from two uninvestigated wild plants: *Centranthus longiflorus* subsp. longiflorus and *Cerinthe minor* subsp. *auriculata*. *European Journal of Integrative Medicine*, *8*(3), 286–292. DOI: 10.1016/j.eujim.2015.12.004.

Zengin, G., Yagi, S., Cziaky, Z., Jekő, J., Yildiztugay, E., Maugeri, A., Russo, C., Cetiz, M. V. & Navarra, M. (2025). Exploring the chemical constituents and biological activities of leaf and twig extracts of two Amygdalus species from Turkey's flora: cell-free, in vitro and molecular docking approaches. *Food Bioscience*, *64*(2), 105869. DOI: 10.1016/j.fbio.2025.105869.

Zengin, G., Yagi, S., Eldahshan, O. A., Singab, A. N., Selvi, S., Rodrigues, M. J., Custodio, L., Dall'Acqua, S., Ponnaiya, S. K. M. & Aly, S. H. (2024). Decoding chemical profiles and biological activities of aerial parts and roots of *Eryngium thorifolium* Boiss by HPLC-MS/MS, GC-MS and in vitro chemical assays. *Food Bioscience*, *61*(1), 104556. DOI: 10.1016/j.fbio.2024.104556.

Zhang, Y., Xiong, H., Xu, X., Xue, X., Liu, M., Xu, S., Liu, H., Gao, Y., Zhang, H. & Li, X. (2018). Compounds identification in semen cuscutae by ultra-high-performance liquid chromatography (UPLCs) coupled to electrospray ionization mass spectrometry. *Molecules*, *23*(5), 1199. DOI: 10.3390/molecules23051199.